effsys EXPAND

Resurseffektiva kyl- och värmepumpssystem
samt kyl- och värmelager

Thermal energy storage with PCM for energy systems in buildings

Korttidslagring av energi med fasändringmaterial för effektiv integrering med värme- och kylsystem i byggnader

Samer Sawalha

Tianhao Xu

June 2018

Energimyndigheten

Förord

The Authors would like to acknowledge the Swedish Energy Agency for funding this research through Effsys Expand program. The authors would also like to thank the project's industrial partners: Danfoss Värmepumpar AB, Energi & Kylanalys, and Vesam.

The authors would like also to thank the students who did their work on certain tasks in the project as part of their degree projects work.

Sammanfattning

Detta projekt undersökte experimenterat prestanda för energilager (TES) med gelerat salthydrat fasändringsmaterial (Phase Change Materials:PCM). Experimentell analys har genomförts på en testbädd som är konstruerad och byggd inom detta projekt. Testbädden experimentella kapacitet täcker brett utbud av värme- och kylanvändningar. Den kan köras inom temperaturområdet -10 till 90°C med en uppvärmningskapacitet på ca 20 kW och en kylkapacitet på ca 10 kW. Testbädden är fullt utrustad med noggranna mätningar som underlättar detaljerad analys av PCM-TES tankens prestanda.

PCM har testats med en testmatris på 29 poäng där varje test tog cirka 10 timmar att genomföra. Testerna gav fullständig karaktärisering av PCM-TES tanken med prestandakarta som kan användas för PCM-TES-dimensionering och effektiv integration i relevanta energisystem. De viktigaste inverkanparametrarna på prestanda för PCM-TES har identifierats och inkluderats i prestandakartan.

Detta projekt undersökte även integrationen av PCM-TES-tanken i värmesystem med luftvärmepump för familjs hus i Sverige. Potentiella besparingar presenteras och systemändringar har föreslagits.

Förutom de redan erhållna forskningsresultaten är testutrustning och analysmetoder (experimentell och modellering) som har upprättats i detta projekt viktiga resultat. Denna kraftfulla forskningsinfrastruktur kan användas i framtiden som en plattform för modellering och testning av nya PCM och TES-tankkonfigurationer.

Analysen som gjorts i detta projekt har presenterats i 3 konferensartiklar, 1 teknisk tidningsartikel och 3 examensarbete rapporter (som ska publiceras inom en snar framtid). Resultaten från projektet kommer också att inkluderas i framtida artiklar i vetenskapliga tidsskrifter inom ramen för doktorandstudierna Tianhao Xu. Doktorsavhandling om ämnet kommer att publiceras i slutet av Tianhoa Xu: s studier, vilket förväntas vara 1-1,5 år från och med nu.

Summary

This project experimentally investigated the performance of thermal energy storage (TES) tank with gelled salt hydrate phase change material (PCM). The experimental analysis has been conducted on a test rig that is designed and built within this project at the Energy Technology Department at KTH. The test rig's experimental capacity covers wide range of heating and cooling/refrigeration applications; it can run in the temperature range of -10 to 90°C with a heating capacity of about 20kW and cooling capacity of about 10 kW. The test rig is fully equipped with highly accurate measurements that facilitate detailed analysis of the PCM-TES tank performance.

The PCM has been tested with a test matrix of 29 points where each test took about 10 hours to accomplish. The tests gave complete characterization of the PCM-TES tank with performance map that can be used for PCM-TES sizing and efficient integration into the relevant energy system/s. The key influencing parameters on the performance of the PCM-TES have been identified and included in the performance map.

This project also investigated the integration of PCM-TES tank into heating system with air source heat pump (ASHP) for single family house in Sweden. Potential savings are presented and system modifications have been suggested.

In addition to the already obtained research results, the testing equipment and the analysis methods (experimental and modelling) that have been established in this project are important outcomes. This powerful research infrastructure can be used in the future as a platform for modelling and testing new PCMs and TES tank configurations.

The analysis done in this project has been included in 3 conference papers, 1 technical magazine paper, and 3 master thesis projects (to be published in the near future). Results from the project will also be included in future journal publications within the frame of the PhD studies of Tianhao Xu. PhD thesis on the topic will be published at the end of Tianhoa Xu's studies, which is expected to be 1-1,5 years from now.

Table of content

Nomenclature

T	Temperature (°C)
$\dot{V}$	Volumetric flow rate ($m^3 \cdot h^{-1}$)
$\dot{Q}$	Thermal power (kW)
Q	Thermal capacity (kWh)
t	Time (h)
V	Volume (m^3)
ρ	Density ($kg \cdot m^{-3}$)
c_p	Specific heat ($kJ \cdot kg^{-1} \cdot K^{-1}$)
k	Thermal conductivity ($W \cdot m^{-1}K^{-1}$)

Subscripts

av	average
in	inlet
out	outlet
loss	heat loss
amb	ambient air
w	water
l	liquid
s	solid

Abbreviations

ASHP	air source heat pump
COP	coefficient of performance
HTF	heat transfer fluids

PCM	phase-change material
PCM-TES	Phase Change Material based Thermal Energy Storage
TES	thermal energy storage

1 Background

Buildings are responsible for about 40% of total energy use in Sweden and Europe. The increasing rate of constructing new buildings and the rate of refurbishment of the large old building stock offer valuable opportunity to introduce highly efficient energy systems.

The IEA Technology Roadmap for Energy-efficient Buildings[1] specifies thermal energy storage (TES) as one of four key technology options for heating and cooling in buildings. Phase Change Material based Thermal Energy Storage (PCM-TES) could replace sensible heat storage solutions. Such an innovative concept utilizes the phase change of a substance to store and release energy at a narrow range of temperature change, resulting in 5-15 times larger storage density than with the commonly used sensible heat storage. This makes it possible to design a compact system that fits in the limited space available in buildings but with much greater storage capacity, thereby allowing for an increased use of renewable energy and waste heat.

An example of an energy system solution with high potential for energy savings by using PCM-TES is an ASHP. The large storage capacity of PCM-TES will allow the ASHP to run during daytime when the outdoor temperature is relatively high and the heating demand is low; therefore, heat is being stored at high system efficiency and heating capacity.

PCM-TES can also be used to shift the load according to electricity prices during the day, so the system is controlled to have longer running time to store thermal energy during the time when the electricity prices are low, thereafter the stored energy can be discharged during the period when the electricity prices are high. This approach can be applied to wide range of energy systems, such as air or ground source heat pumps.

There are several parameters that influence the performance of PCM-TES tanks, such as: volume flow rate, pressure drop, heat transfer, encapsulation geometry, etc. Therefore, it is essential to use computer modelling to optimize the PCM-TES tank design and use experimental analysis to characterize its performance. This will give guidelines of how to integrate and control the PCM-TES tank in an optimized way into energy systems.

Researchers at the Energy Technology Department at KTH have good experiences over the years working with PCM's, thermal storage, and energy systems. However, the research infrastructure at the department lacked an experimental test rig for testing and

[1] IEA Technology Roadmap for Energy efficient Buildings: Heating and Cooling Equipment, 2011

characterizing the performance of real scale PCM-TES tanks at wide range of operating temperatures. Such test rig combined with the computer modelling platform will be powerful tools for detailed characterization and optimization of the performance of PCM-TES tanks.

2 Implementation

The investigations in this project have been based on experimental analysis and computer simulation modelling. In parallel, extensive literature review has been continuously conducted.

A test rig has been designed and built at the Energy Technology Department at KTH to cover wide range of heating and cooling/refrigeration applications. The test rig can run in the range of -10 to 90°C with a heating capacity of about 20kW and cooling capacity of about 10 kW. The test rig is fully equipped with highly accurate measurements that facilitate detailed analysis of the PCM-TES tank performance. Three categories of parameters are measured to characterize the performance of the PCM-TES tank: temperatures, the volumetric flow rate and the pressure drop.

The TES tank has been designed in this project to contain the PCM rods that have been provided by one of our project partners. The tank design assures uniform heat transfer fluid distribution over the PCM rods and facilitates access to measuring points inside the tank and the PCM rods.

Simplified one dimensional model has been conducted using calculations in Excel and the software Engineering Equations Solver (EES). The results were compared to the experimental findings. The two dimensional model has been done using the commercial CFD software ANSYS FLUENT.

The PhD student Tianhao Xu had the tasks of conducting the research activities in the project. Project leader and principal supervisor has been Associate Professor Samer Sawalha. Prof. Viktoria Martin and Assistant Professor Justin Chiu at the Energy Technology department are experts on PCMs and provided feedback on project activities and results. Piscopiello Salvatore has been employed as research engineer in the project for few months at the project start and helped in designing the test rig. Dr. Muhammad Hamayun Maqbool has been employed for few months in the project and helped in instrumenting the system and coordinating the build-up of the test rig in our laboratory. Loris Tomasi is an exchange student from Italy who ran the first group of test points in the test matrix. Konstantinos Papiris and Hasnain Raza have been, and will continue, working on modelling tasks in the project as part of the master thesis.

Our industrial partners provided almost all materials and equipment necessary to build the test rig and PCM-TES tank. They also provided feedback on every stage of the project, starting from the design phase, during the project progress, and on the research results.

3 Results

The results from the work in this project are summarized in the following sections which represent the key research blocks in the project: experimental analysis, modelling of PCM-TES tank, and modelling analysis of energy system with integrated PCM-TES tank.

3.1 Test rig design and build up

3.1.1 Test rig description and deatures

The test rig has been designed and built to cover wide range of heating and cooling/refrigeration applications. The test rig can run in the range of -10 to 90°C with a heating capacity of about 20kW and cooling capacity of about 10 kW. Schematic of the test rig is presented in Figure 1.

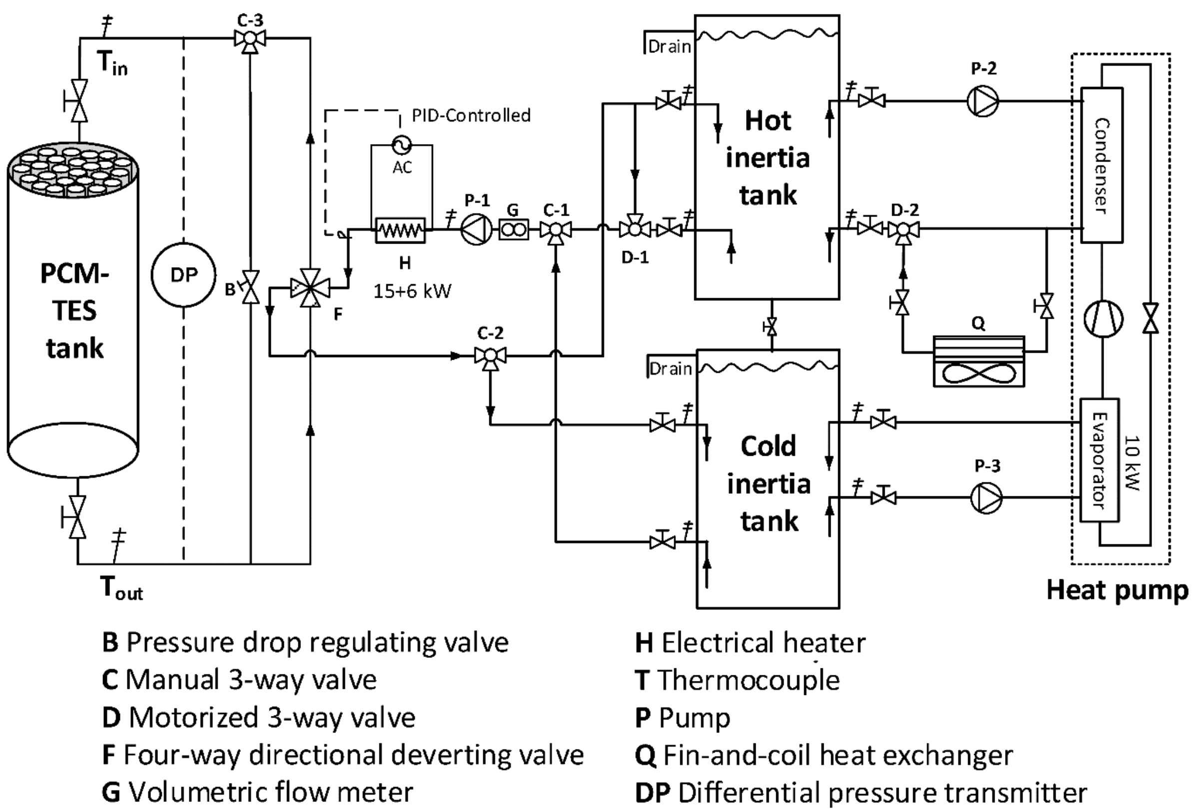

Figure 1: The schematic of the PCM-TES testing facility

The following are main features of the test rig:

- Maintain constant supply temperature of the heat transfer fluid (HTF) to the PCM-TES tank.
- Vary the flow rate of HTF through the PCM-TES tank, up to 5 m^3/hour can be reached.
- Allow for horizontal and vertical alignment of the PCM-TES tank.
- Possibility to reverse the flow direction through the PCM-TES tank with the aid of 4-way valve

The key components in the test rig are a PID-controlled electrical heater (H in Figure 1) that facilitates maintaining constant supply temperature to the PCM-TES tank. A fin-and-coil heat exchanger (Q in Figure 1). A water-to-water heat pump that can provide heating to one of the inertial tanks and provide cooling to the other. The volume of the inertial tanks is 1 m^3 each. A 4-way valve (F in Figure 1) enables switching flow direction of the HTF through the PCM-TES tank. A pressure-drop regulating valve (B in Figure 1) allows stabilizing the desired temperature of supplied HTF before pumping it into the PCM-TES tank, this is essential when preparing for testing.

3.1.2 Instrumentations

The test rig is fully equipped with highly accurate measurements that facilitate detailed analysis of the PCM-TES tank performance. Three categories of parameters are measured to characterize the performance of the PCM-TES tank: temperatures, the volumetric flow rate and the pressure drop. Temperatures are measured using total of 20 T-type thermocouples; two thermocouples are placed at the inlet and outlet of the tank (T_{in} and T_{out} in Figure 1) and the rest were placed inside the tank for measuring HTF and PCM temperatures. The temperatures in the tank have been examined to show a mean discrepancy within 0,05°C comparing to a precision digital thermometer in the temperature span from 30°C to 70°C by every two kelvins

The volumetric flow rate is measured by a magnetic flowmeter, Yokogawa RXF, with a relative measurement error of $\pm$0,5 %. The pressure drop across the tank is measured by two ports at the inlet and outlet connecting to a differential pressure transmitter, Yokogawa EJA 110A, with an error of $\pm$0,055%.

3.1.3 Thermal energy storage tank

The initial design of the tank was supposed to reflect the design used in practice with the selected type of PCM. Schematic of the initial tank design is presented in Figure 2.

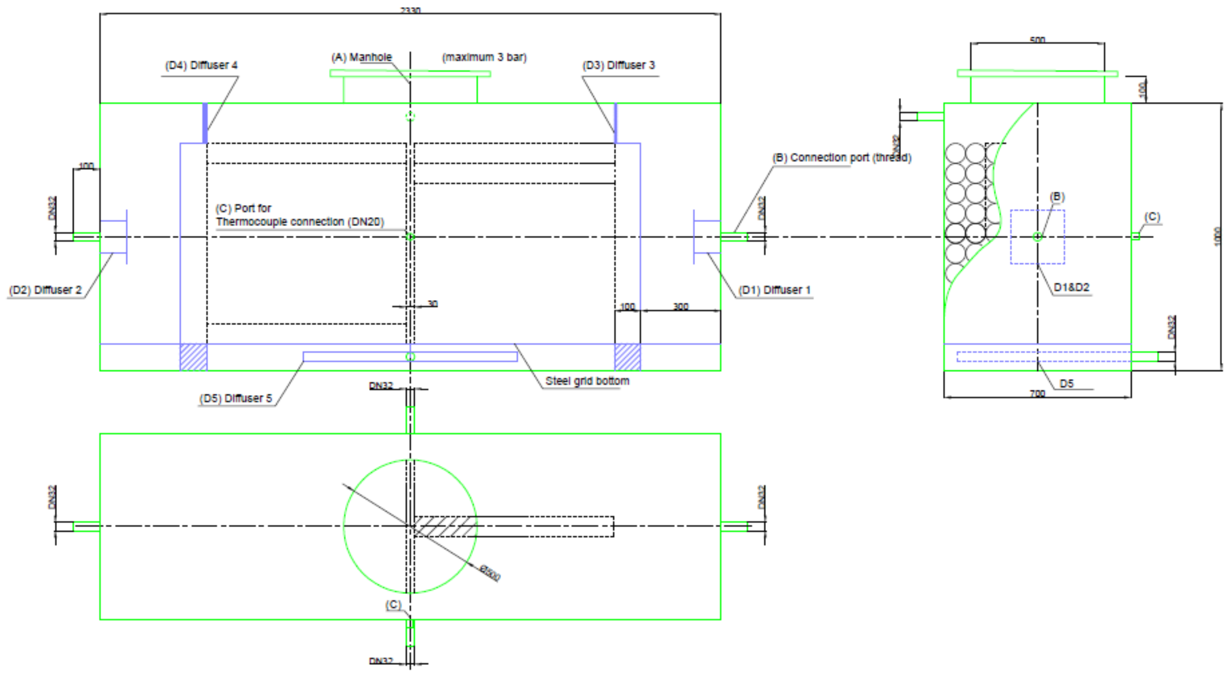

Figure 2: Schematic of initial design of TES tank

The tank has the shape of rectangular cuboid with two rows of PCM rods placed in the HTF flow direction. The design was abandoned due to large manufacturing cost.

The design that has been adapted in the project used standard cylindrical stainless steel pipe, Type 316, with internal diameter of 600mm. Schematic of the TES tank is in Figure 3.

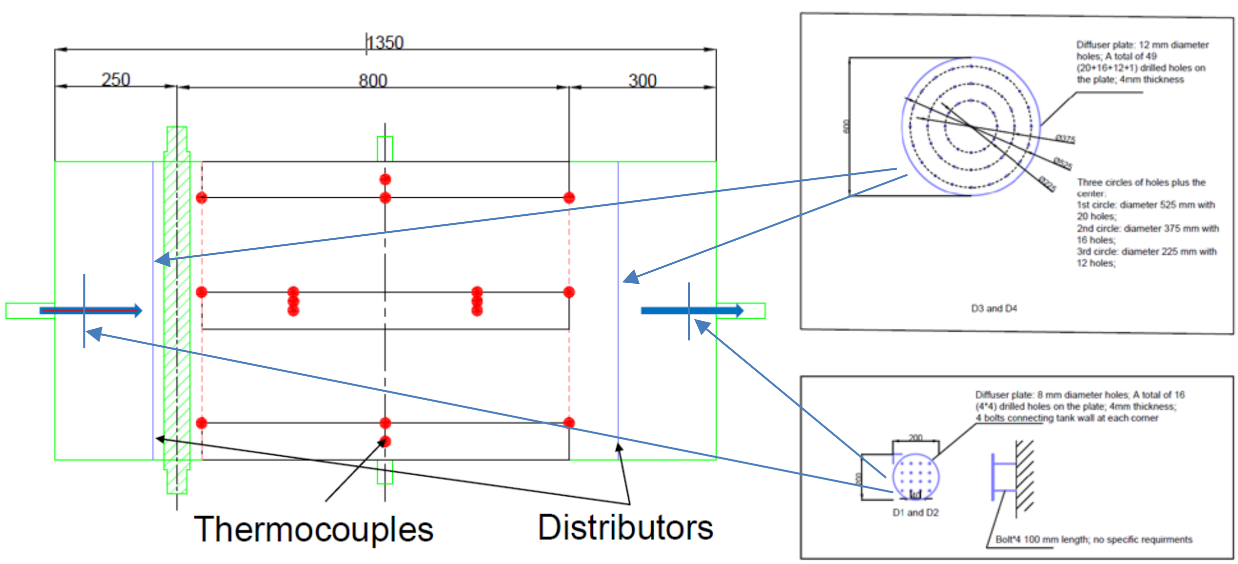

Figure 3: Schematic of the adapted TES tank design

The pipe (i.e. tank) has a length of 800mm which accommodates a single row of PCM rods that have a length of 750mm. As can be seen in Figure 3, the inlet and outlet ports of the tank have been designed with restriction plate at the flow entrance to the tank, which is followed by a plate with large number of holes to achieve uniform flow distribution around the PCM rods. The inlet and exit sections of the TES tank have identical design to allow for reversing the flow direction.

The TES tank is filled with as many PCM rods as possible, 50 rods, and covered by an insulation layer with a thickness of 19mm, as can be seen in Figure 4. The PCM-TES tank can be either horizontally or vertically placed to study the effects from the HTF direction.

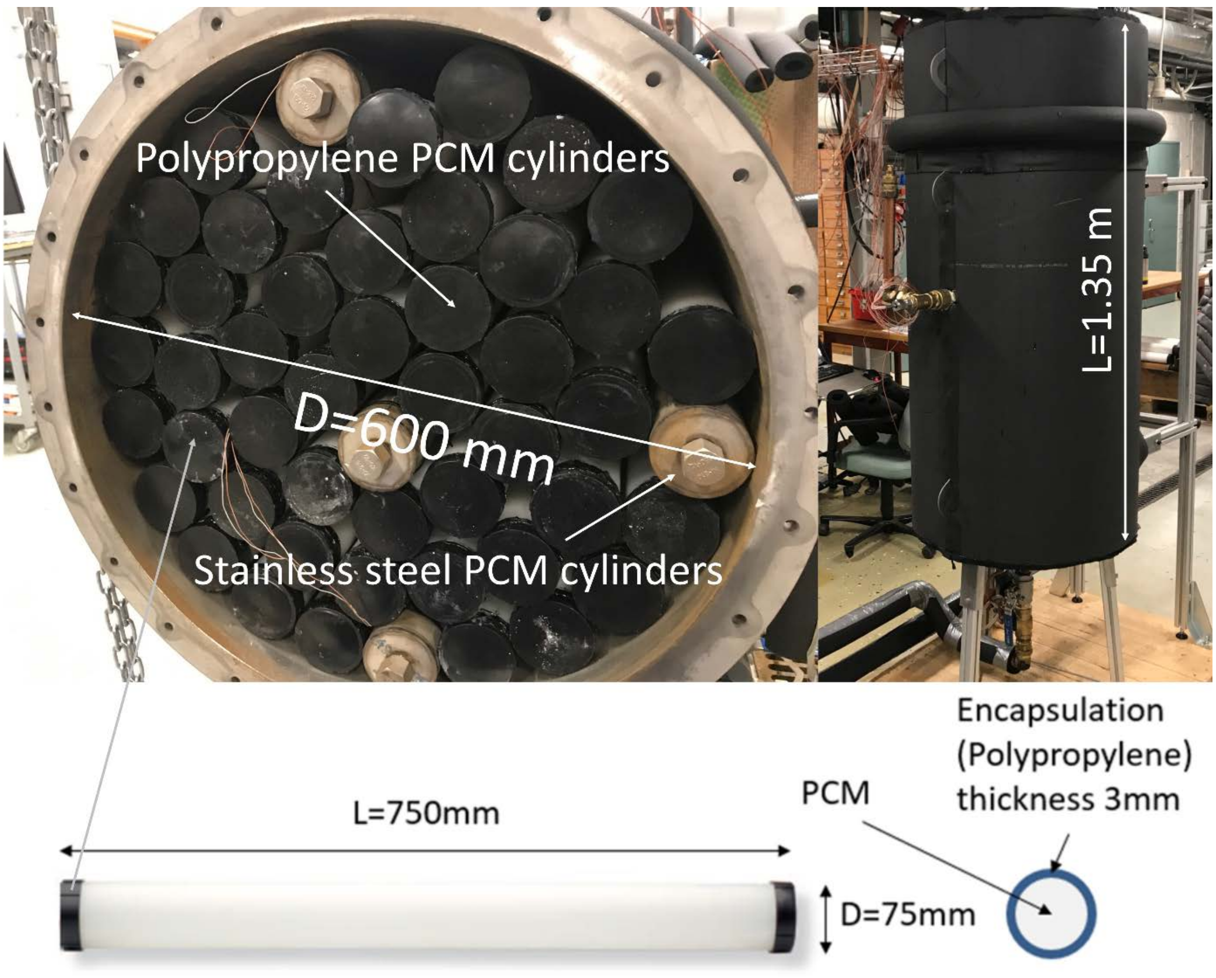

Figure 4: The PCM-TES tank and encapsulated PCM cylinders

3.1.4 PCM characterstics

A common way for PCM containment is to macro-encapsulate PCMs in certain shapes of plastic or metallic containers[2]. The encapsulation is essential for providing good isolation of PCMs from the HTF, as well as creating flexibility for maintaining and reloading of the TES unit with PCMs. For salt hydrates, proper encapsulation prevents them from losing water content, dissolving in water and therefore creating corrosive solution that can damage the hydraulic loop. Macro-encapsulation differs in the shape and size according to the manufacturers. Although spherical containers for PCMs are proved to have the highest heat transfer rate compared to other shapes[3], using plastic cylinders as an alternative for macro-encapsulation is considered as one of the most cost-effective solutions[4].

In the present study, a cylindrical macro-encapsulated PCM product was tested in the aforementioned experimental apparatus. The tested PCM is a commercial product named ClimSel C48, and the thermo-physical properties of it are listed in Table 1.

Table 1: Thermo-physical properties of ClimSel C48

Parameter	Value
Density (ρ)	1300 $kg{\cdot}m^{-3}$
Phase-change temperature (melting)	46 to 52 ^{o}C
Phase-change temperature (solidification)	48 to 43 ^{o}C
Latent heat of fusion (40^{o}C to 55^{o}C)	180 kJ·kg^{-1}
Thermal conductivity: solid (k_s)	0.76 $W{\cdot}m^{-1}K^{-1}$
Thermal conductivity: liquid (k_l)	0.53 $W{\cdot}m^{-1}K^{-1}$

This PCM stores most of the latent heat in the temperature span between 46 to 52°C in the melting process and releases the majority between 48 to 43°C when solidified, according to the specific heat curve provided by the manufacturer[5], the enthalpy

[2] Salunkhe, P.B. and P.S. Shembekar, A review on effect of phase change material encapsulation on the thermal performance of a system. Renewable and Sustainable Energy Reviews, 2012. 16(8): p. 5603-5616.
[3] Wei, J., et al., Study on a PCM heat storage system for rapid heat supply. Applied Thermal Engineering, 2005. 25(17): p. 2903-2920.
[4] Regin, A.F., S.C. Solanki, and J.S. Saini, Heat transfer characteristics of thermal energy storage system using PCM capsules: A review. Renewable and Sustainable Energy Reviews, 2008. 12(9): p. 2438-2458.
[5] Climator. 2018; Available from: http://climator.com/wp-content/pdf/Prodblad_Climsel_C48_4.1.pdf.

temperature diagram is presented in Figure 5. This PCM is based on gelled salt hydrates to prevent the phase segregation during the solidification.

The melting and solidification temperature range for ClimSel C48 suits well the temperature levels for space heating system which is investigated in this project.

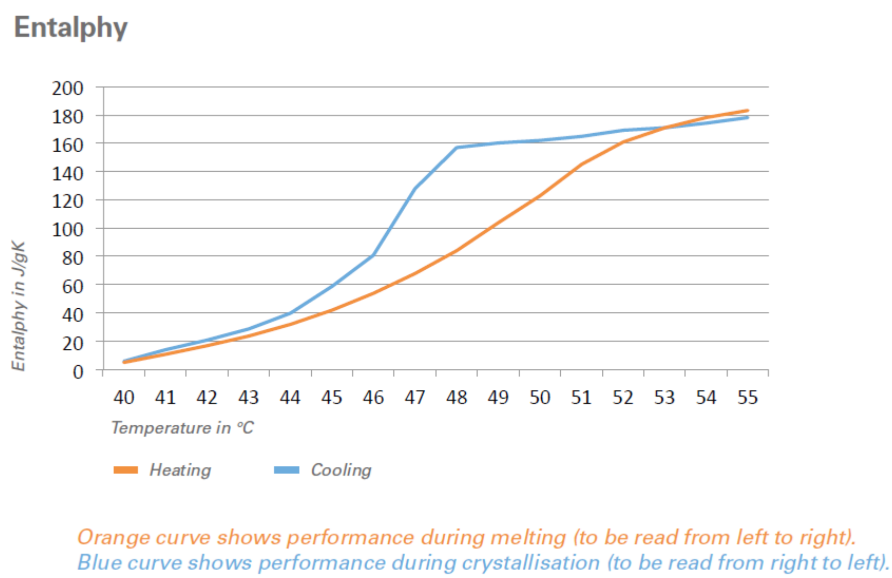

Figure 5: Enthalpy temperature diagram of ClimSel C48[6]

In Figure 4, the dimension of the PCM encapsulation is illustrated; the encapsulation is made of polypropylene and the thickness of that is 3 mm. As shown in Figure 4, the tank is loaded with 50 PCM cylinders, the total mass of contained PCM is 154 kg. It is worth noticing in Figure 4 that four PCM cylinders are encapsulated in stainless steel rods Type 316. They are customized in the same dimension as the plastic ones but with temperature measuring points inserted in thermowells, which was not possible to implement in the original plastic cylinders encapsulating the PCM. The purpose of such configurations is to measure the temperature evolution of encapsulated PCMs in different positions of the tank during phase-changing processes. Positions of most of the thermocouples inside the PCM-TES tank can be observed in Figure 3.

[6] Climator. 2018; Available from: http://climator.com/wp-content/pdf/Prodblad_Climsel_C48_4.1.pdf.

3.2 Experimental analysis

The experiments focused on characterising the performance of the PCM-TES tank by varying volume flow rate and temperature of the HTF in charging and discharging operations. The horizontal and vertical alignment of PCM-TES tank has also been studied. The key parameters that have been used to characterize the performance of PCM-TES tank are: the charging time, discharging time, stored and released energies. The tests have been conducted at different initial temperatures of the PCM-TES tank.

Performance maps have been developed which facilitate selecting the optimum operating conditions of the PCM-TES tank in charging and discharging operations.

3.2.1 Test matrix

The test points used to characterize the performance of the PCM-TES tank are listed in the test matrix in Table 2. Total of 29 points where tested, each test point took about 10 hours to conclude.

Table 2: Detailed test matrix of C48

Charging			Discharging		
Alignment	HTF supply temperature (°C)	HTF volume flow rate (m^3/hr)	Alignment	HTF supply temperature (°C)	HTF volume flow rate (m^3/hr)
Horizontal	55 (Initial at 35)	0,5	Horizontal	30 (Initial at 55)	0,5
		1,5			1,5
		4,0			4,0
	55 (Initial at 40)	1,0		35 (Initial at 55)	0,5
		1,5			1,0
		2,5			1,5
	58 (Initial at 35)	1,5			2,5
	60 (Initial at 35)	1,5			4,0
		4		40 (Initial at 55)	0,5
					1,5
Vertical	55 (Initial at 35)	1,5	Vertical	35 (initial at 55)	0,15
		4			0,25
	58 (Initial at 35)	1,5			0,5
	60 (Initial at 35)	1,5			1,0
					1,5
					4,0

3.2.2 Experimental procedure and balancing equations

At the start of each charging/discharging test the temperature of the PCM-TES tank was uniformly maintained at certain temperature; i.e. initial temperature. Valve C-3 in Figure 1 is configured to divert the HTF flow. The charging/discharging test starts when the by-pass valve C-3 is fully closed and the HTF fluid with the required temperature is directed to follow through the PCM-TES tank. The test was considered complete when the outlet HTF temperature levelled off.

The horizontal alignment of the PCM-TES tank was tested in the first place followed by the vertical position testing, the key results are presented in the following section.

The thermal power (in kW) is calculated by the heat balance of the HTF over the TES unit as given in Equation (1).

$$\dot{Q}_{TES} = \rho_{HTF} \dot{V}_{HTF} c_{p,HTF} \left(T_{TES,in} - T_{TES,out} \right)_{TES} \quad (1)$$

The thermal capacity is an accumulation of the thermal power over a period of time (from t_1 to t_2), which represents the total amount of heat content being stored or released during charging or discharging. The thermal capacity of the PCM-TES tank is calculated based on Equation (2).

$$Q_{TES} = \int_{t_1}^{t_2} \dot{Q}_{TES} \, dt \quad (2)$$

Where the thermal capacity, Q_{TES}, constitutes of three parts: the capacity stored or released by the PCM mass, capacity stored or released by the HTF volume in the tank, and heat loss from the tank to the ambient. The heat balance is expressed in Equation (3).

$$Q_{TES} = \int_{t_1}^{t_2} (\dot{Q}_{PCM} + \dot{Q}_{loss}) dt + Q_{HTF} \quad (3)$$

The heat loss of the PCM-TES tank, $\dot{Q}_{loss}$, is experimentally obtained by maintaining the tank at certain temperatures over a long period and calculating the heat balance. Heat loss to the ambient was measured from 25 to 60°C where a global heat loss coefficient was obtained by linearly correlate the heat loss with the temperature difference between the unit and the ambient, see Equation (4). UA_{TES} for this unit is 7.4 W/K.

$$\dot{Q}_{loss} = UA_{TES} (T_{TES,av} - T_{amb}) \quad (4)$$

During the charging process, part of the heat capacity is stored as sensible heat in the HTF volume in the tank, due to the increased HTF temperature comparing to the initial temperature at the start of the test. This part of sensible heat is subsequently released in the discharging process by lowering the temperature of the HTF in the tank. The transient amount of charged or discharged sensible heat is calculated by averaging the HTF temperature in the tank throughout distributed temperature measuring points in the tank, as given in Equation (5).

$$Q_{HTF} = \rho_{HTF} V_{HTF,TES} c_{p,HTF} \left(T_{HTF,av,t_2} - T_{HTF,av,t_1} \right) \quad (5)$$

The parameters required to calculate the thermal capacity going to PCMs (Q_{PCM}) are obtained from Equations (2), (4), and (5), then substituted in Equation (3).

3.2.3 Experimental results

Horizontal alignment tests

Charging

The PCM C48 stores most of latent heat in the temperature span between 46 to 52 °C; therefore, the HTF supply temperatures tested are 55, 58 and 60°C. The effect of the volumetric flow rate of the HTF is tested for 1,0, 1,5, and 2,5 m^3/hr. Example of the results for the varying HTF supply temperature is presented in Figure 6. In this test the volume flow rate of the HTF is kept at 1,5 m^3/hr and the initial temperature of the PCM-TES tank was 35°C.

The continuous and dashed lines represent the stored total and PCM thermal capacity, Q_{TES} and Q_{PCM} respectively, while the dotted lines represent the mean PCM temperature at the center of the four stainless steel tubes ($T_{PCM, av}$).

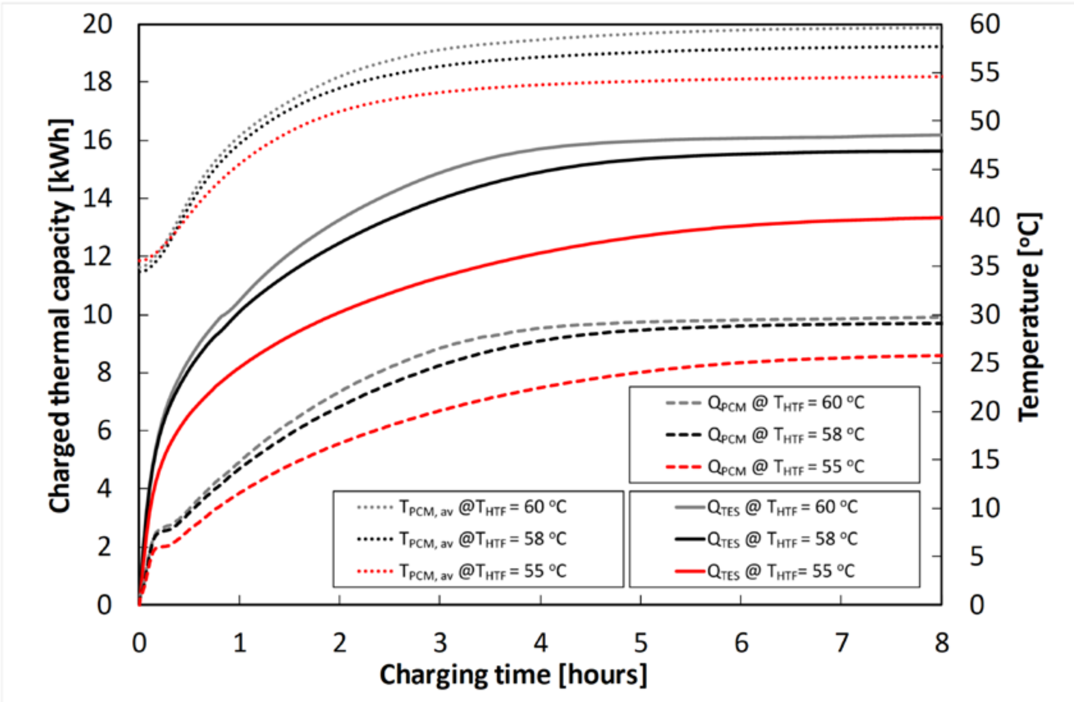

Figure 6: The evolution of PCM average core temperature and stored thermal capacity (total/Q_{TES} and Q_{PCM}) with different HTF supply temperature (55, 58, and 60 °C). Initial test temperature is 35°C and volume flow rate of HTF is 1,5 m^3/hr.

It can be observed in Figure 6 that higher HTF supply temperature results in increased $T_{PCM,\ av}$, Q_{TES} and Q_{PCM}. Fully-developed Q_{TES} increased from 13,7 to 16,4 kWh and Q_{PCM} increased from 8,9 to 10,1 kWh by increasing the HTF supply temperature from 55 to 60°C. The increase in charging capacity with increasing HTF supply temperature is due to storing sensible energy in the PCM rods after achieving complete melting.

It can also be observed in Figure 6 that the charging time can be significantly reduced with increasing HTF supply temperature. For instance, it takes 5,6 hours for charged Q_{PCM} to reach 8 kWh with HTF supply temperature of 55°C but only 3,1 hours with that of 58°C. However, further increasing the HTF supply temperature to 60°C only reduces this time to 2,7 hours. The improving effect of increasing HTF supply temperature is also found on the evolution of PCM temperature (dotted lines), where the PCM is completely melted in shorter time with higher HTF supply temperature; i.e. the PCM core temperature reaches 52°C.

General observations that have also been evident in the rest of the charging tests is that increasing HTF temperatures accelerates the charging process, where the temperature difference between HTF and the PCM melting temperature span should be large enough to accomplish quick melting; however, it shouldn't be too large because the effect on shortening the melting time becomes smaller. For instance, the charging time is much shorter for HTF supply temperature of 58°C compared to 55°C, while the difference is smaller between 58 and 60°C.

The influence of varying the HTF volume flow rate on the charging time is presented in the sample test in Figure 7. The initial PCM-TES tank temperature in this test is 40°C and the HTF supply temperature is 55°C.

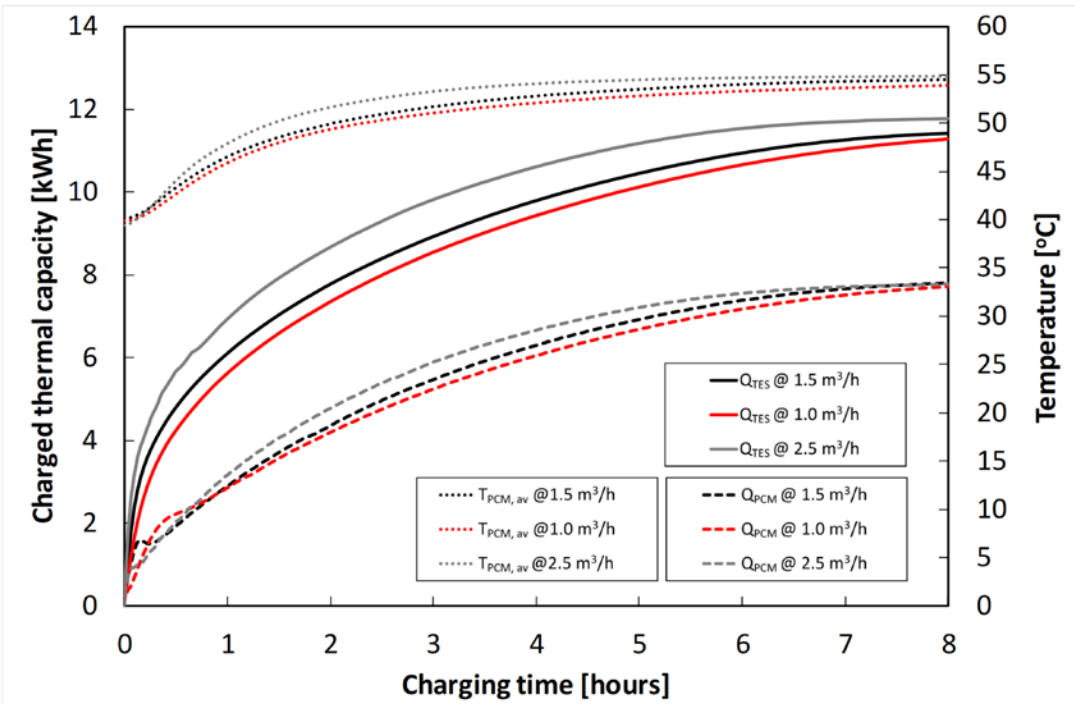

Figure 7: The evolution of PCM average core temperature and stored thermal capacity (total/Q_{TES} and Q_{PCM}) with different HTF volume flow rates (1, 1,5 and 2,5 m^3/hr). Initial test temperature is 40°C and supply temperature of HTF is 55°C.

As can be observed in Figure 7, gray lines representing the test with a volumetric flow rate of 2,5 m^3/h increase the most rapidly; Q_{PCM} reach 7 kWh at 4,5 hours. However, with 1,0 m^3/h condition Q_{PCM} reach 7 kWh at 5,6 hours. Eventually, all lines end up with approximately the same values because these three tests were run with the same initial PCM-TES tank and HTF supply temperatures (40 and 55°C respectively).

The shorter charging time with increasing volume flow rate of HTF is attributed to increasing convective heat transfer coefficient at the rods surfaces. The pressure drop across the tank was not presented in a figure because the value was negligible at all tests. In this test for instant, the value ranged between 1 Pa (0,5 m^3/hr) to 10 Pa (4,0 m^3/hr).

General observations from these, and the rest of the charging, rests are that the effect of HTF supply temperature on shortening the charging time is more prominent than increasing the volume flow rate. This will be presented and discussed later in this chapter in the performance map sub-section.

Discharging

The PCM C48 solidifies in the temperature span of 48 to 43°C; therefore, lower HTF supply temperatures were tested; 30, 35, and 40°C. The effect of the volumetric flow rate of the HTF was also tested for 0,5, 1,5, and 4 m^3/h. Example of the results for the varying HTF supply temperature is presented in Figure 8. In this test the volume flow rate of the HTF is kept at 1,5 m^3/hr and the initial temperature of the PCM-TES tank was 55°C.

It can be observed in Figure 8 that Q_{TES} and Q_{PCM} increase with decreasing HTF supply temperature as more sensible heat is retrieved from the PCM and the HTF volume in the tank. Also it can be observed that the discharging process is accelerated with lower HTF supply temperature. For instant, it takes about 4,6 hours to discharge 8 kWh of Q_{PCM} with HTF supply temperature of 35°C, but it takes only 2,5 hours with 30°C. With HTF supply temperature of 40°C it was not possible to recover 8 kWh. $T_{PCM,av}$ decreases more rapidly to 43°C with reduced HTF supply temperatures as well; less than 1 hour with 30°C while it takes about 3 hours with 40°C.

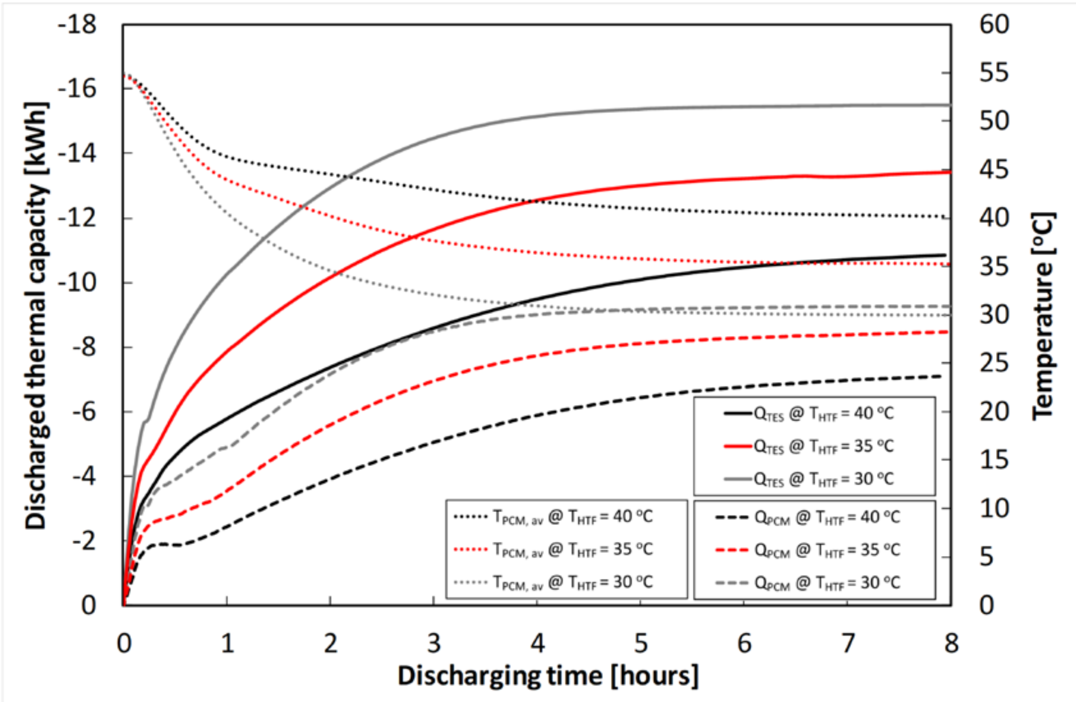

Figure 8: The evolution of PCM average core temperature and released thermal capacity (total/Q_{TES} and Q_{PCM}) with different HTF supply temperature (30, 35, and 40°C). Initial test temperature is 55°C and volume flow rate of HTF is 1,5 m^3/hr.

The influence of varying the HTF volume flow rate on the discharging time is presented in the sample test in Figure 9. The initial PCM-TES tank temperature in this test is 55°C and the HTF supply temperature is 30°C.

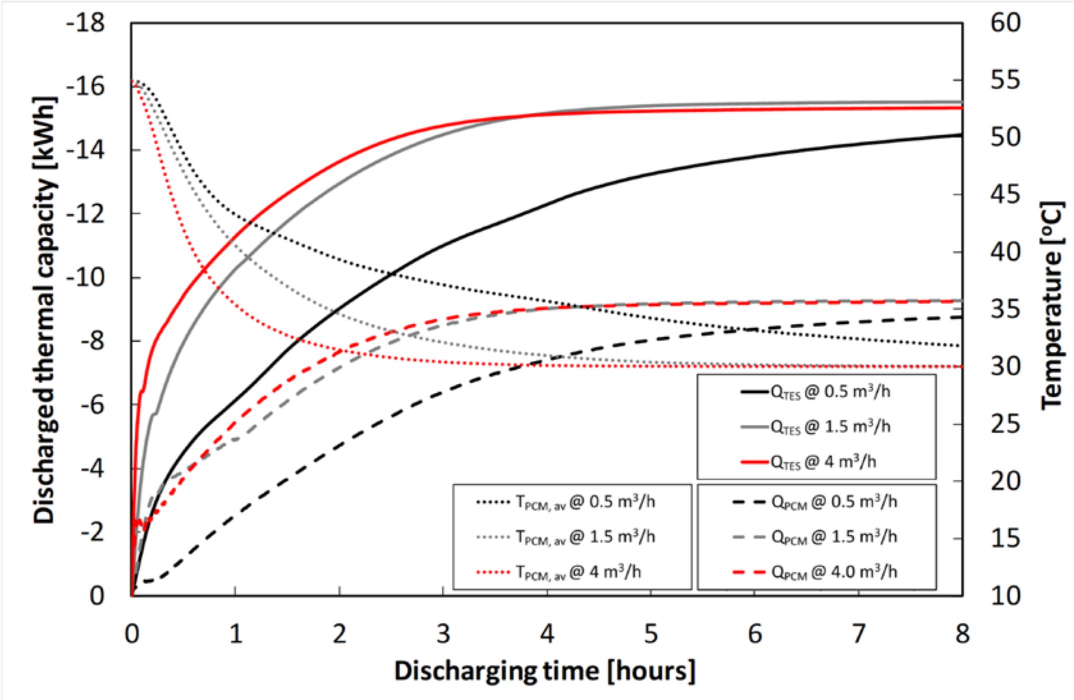

Figure 9: The evolution of PCM average core temperature and released thermal capacity (total/QTES and QPCM) with different HTF volume flow rates (0,5, 1,5, and 4 m3/hr). Initial test temperature is 55°C and supply temperature of HTF is 30°C.

It can be observed in the plots in Figure 9 that the differences in discharging time between flow rate of 1,5 and 4 m^3/hr are small; however, with 0,5 m^3/hr the Q_{TES} and $T_{PCM,av}$ the lines do not become flat within the test period of 8 hours. This is due to the uneven distribution in the PCM-TES tank occurred with a relatively small flow rate of HTF and thus the top area of tank did not reach the supply HTF temperature within this timespan.

General observations from these, and the rest of the discharging, tests are that lowering HTF supply temperature and increasing its volume flow rate will shorten the discharging time. The flow rate of the HTF must be high enough to accomplish uniform distribution of HTF in the PCM-TES tank. This will be presented and discussed later in this chapter in the performance map sub-section.

Performance map

The performance data of the ClimSel C48 PCM rods were obtained according to the test matrix in Table 2 and used to generate a performance map of the PCM. Parameters that are included in the performance map in Figure 10 and Figure 11 are:

- Initial temperature of the PCM-TES tank: can be identified with the line type and grouped with HTF supply temperature
- HTF supply temperature: can be identified with the line type
- Volume flow rate of HTF: can be identified by the line colour
- Percentage of total charging/discharging capacity: can be identified by the marker type

Percentage of total charging/discharging capacity represents the partial-load status in every single testing condition. This is defined as φ to describe the transient storage and recovery of latent heat in PCMs compared to the theoretical storing/recovering capacity of this product according to the specific curve provided by the PCM manufacturer. It is calculated according to Eq. (6). Three values are used in the performance map plots: 75 %, 90 % and 99%. For example, at the moment (t_1) when φ equals to 75% in a charging process, PCMs store 75% of its theoretical heat storage capacity.

$$\varphi = \int_0^{t_1} Q_{PCM} \,/\, Q_{PCM,theo} \tag{6}$$

Using the different parameters in the performance maps it is possible to obtain the charging and discharging capacity and time which are essential information for designing PCM-TES systems with optimal performance.

For a condition with initial PCM-TES tank temperature of 35°C and a need to charge 99% of the theoretical capacity, it can be observed in Figure 10 that the shortest charging time is 3,7 hours with HTF supply temperature of 60°C and flow rate of 4 m^3/h. The charging time is; however, much higher and equal 6,8 hours with HTF supply temperature of 55°C with 1.5 m^3/h. It can also be observed in Figure 10 that the difference in charging time and capacity is not so great between the cases of HTF supply temperatures of 58 and 60°C.

It is clear in Figure 10 that low volume flow rates which may result in uneven distribution of HTF in the TES tank must be avoided, for instance the case of 0,5 m^3/hr.

According to Figure 10, the charging time increases steeply from 75 % to 99 % on an individual testing condition. For the test of 35 to 55°C with 1,5 m^3/h, the charging time can be shortened from 6,8 hours to 3,0 hours if only 75 % of the thermal capacity is aimed to be stored instead of 99 %. This saving in time of partial-load charging conditions are also found in other testing conditions in the map, in average about 50 %

less charging time is found for 75 % capacity compared to 99 %. Therefore, a timesaving charging strategy of the studied PCM-TES tank could be developed based on the realistic demands of the charged thermal capacity.

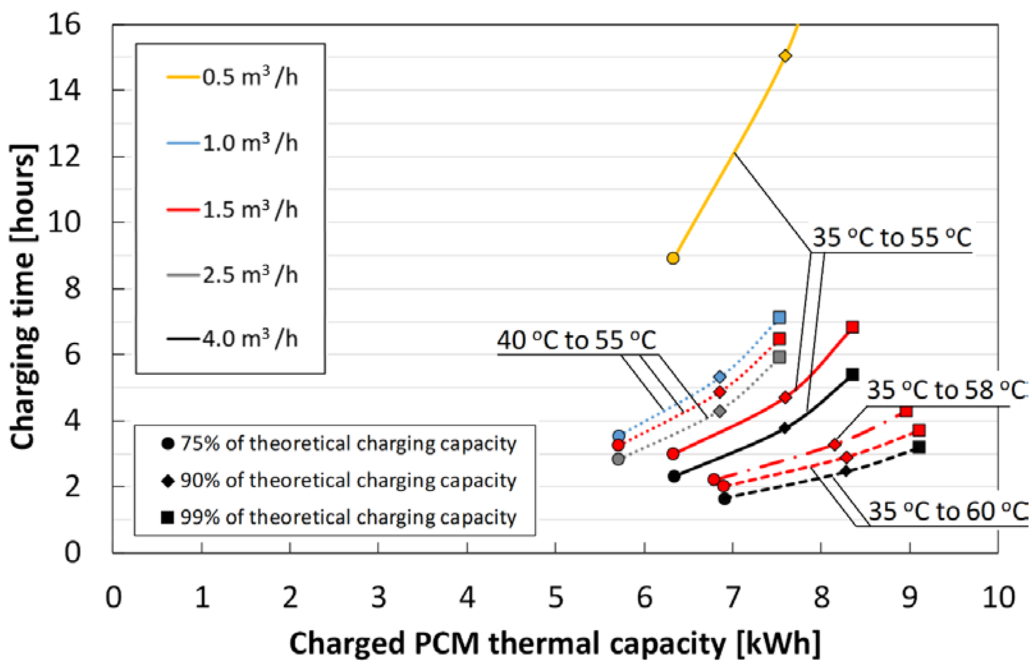

Figure 10: Performance map for charging operation.

A similar map is generated for discharging processes and plotted in Figure 11. For a condition with initial PCM-TES tank temperature of 55°C and a need to recover 99 % of the theoretical capacity, it can be observed in Figure 11 that the shortest discharging time is 3,4 hours with HTF supply temperature of 30°C and flow rate of 4 m^3/h. The discharging time is; however, 4,9 hours with HTF supply temperature of 35°C with 1,5 m^3/h.

The relatively steep increase in charging time at high discharging capacity percentage is also observed in Figure 11 similar to the observation in the charging performance map.

It can be noticed in the map that for the testing conditions with HTF supply temperatures of 40^{o}C is was not possible to recover 99 % of the declared capacity. The test on this temperature range with 0,5 m^3/hr couldn't recover up to 90% of the capacity because of the uneven distribution of the HTF in the PCM-TES tank.

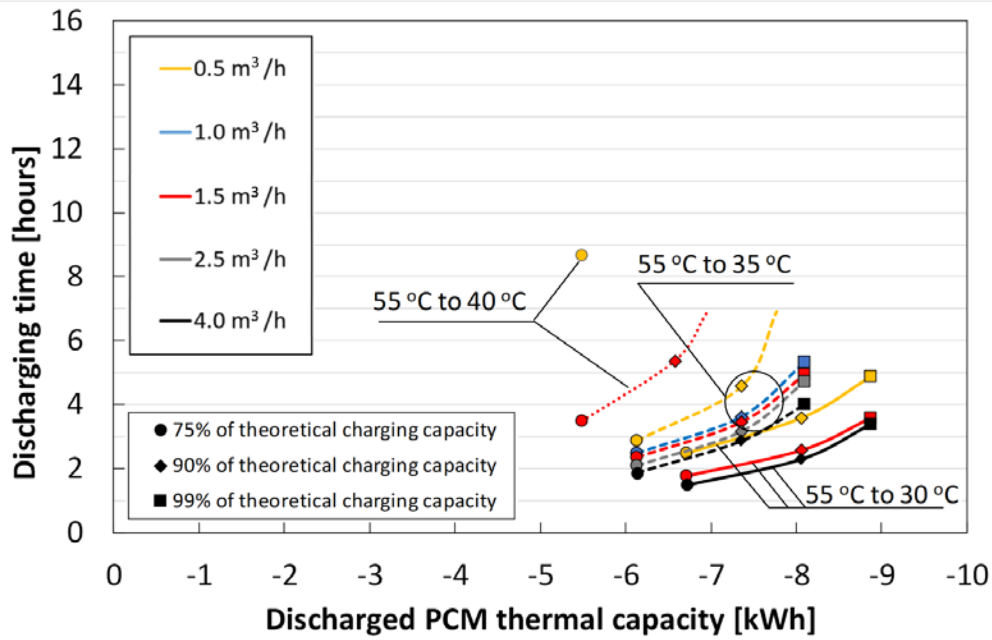

Figure 11: Performance map for discharging operation.

The charging and discharging performance maps show that to achieve the shortest charging/discharging time the HTF supply temperature should be as high as possible during charging and as low as possible during discharging with the highest volume flow rate. However, increasing the HTF supply temperature for charging will increase the condensation temperature of a heat pump if the heating is provided by the condenser; thus decreasing the heating COP. On the other hand, decreasing the HTF temperature for discharging lowers the outlet temperature from the PCM-TES tank and therefore decreases the surface temperature of a radiator if the discharged heat directly provides heating to the space. Increasing the HTF volume flow rate will require increasing pumping power.

Therefore, further optimization of the operating conditions of the PCM-TES tank is needed which should take into account the energy use of the energy system where the PCM-TES tank is integrated into.

Vertical alignment tests

The test points for the vertical alignment in the test matrix in Table 2 have been accomplished. Similar analysis to the horizontal alignment which was presented earlier in this chapter has been conducted. The key differences between vertical and horizontal alignment tests are that:

- Different PCM temperature regime in cylinders were observed which indicate natural convection inside the PCM rods in the vertical alignment

- and the HTF volumetric flow rate can be reduced below 0,5 m^3/hr in vertical alignment while maintaining a good flow distribution of HTF in the PCM-TES tank.

Performance maps have been generated for the vertical alignment similar to the case of the horizontal. The figures and the details of the maps are not presented in this report, but the performance characteristics in the maps are explained in the following points:

- The influence of the supply temperature on stored capacity, released capacity, and charging/discharging time in vertical alignment has been similar to horizontal alignment that was presented in Figure 10 and Figure 11.
- However, the effect of varying the HTF flow rate was less noticeable in the vertical alignment. It was also noticed that it is possible to run at quite low HTF volume flow rates, down to 0,15 m^3/hr, without degrading the performance of the PCM-TES tank compared to high flow rates at the same HTF supply temperature. This is mainly due to the diminished effect of HTF stratification in the TES tank when vertically aligned.

In this section the analysis of the differences in temperature distribution inside the rods in horizontal and vertical alignments will be presented.

Temperature profile analysis: vertical vs. horizontal during charging

The tested PCM is a commercial gelled salt hydrate. By gelling, a tight structure is formed to the liquid PCMs through the cross-linking of the additives and make them a more viscous material[7]. Some previous studies show that a good agreement between the simulation and experimental results has been obtained through models which only consider heat conduction in gelled PCMs [8,9].

The stainless steel PCM cylinders were mounted with temperature sensors in thermowells to measure the temperatures inside the rods at different positions. The temperature measurements, T_{pcm1} and T_{pcm2}, inside a PCM rod in the horizontal alignment of the tank resulted in the plots in Figure 12. The test conditions are with HTF supply temperature of 55, 58, and 60°C.

[7] Lane, G., Solar heat storage: Latent heat materials. Volume II. Technology. 1986, Dow Chemical Co., Midland, MI.
[8] aito, A., et al., On the heat removal characteristics and the analytical model of a thermal energy storage capsule using gelled Glauber's salt as the PCM. International Journal of Heat and Mass Transfer, 2001. 44(24): p. 4693-4701.
[9] Chiu, J.N.W. and V. Martin, Submerged finned heat exchanger latent heat storage design and its experimental verification. Applied Energy, 2012. 93: p. 507-516.

A crossing behavior between T_{pcm1} and T_{pcm2} is observed in Figure 12 among all the test conditions, in which T_{pcm1} surpasses T_{pcm2} after both of them reach values above 52°C. By this temperature, the PCM is considered completely melted at the center and the convection of the PCM in liquid phase results in the small temperature gradient between T_{pcm1} and T_{pcm2}.

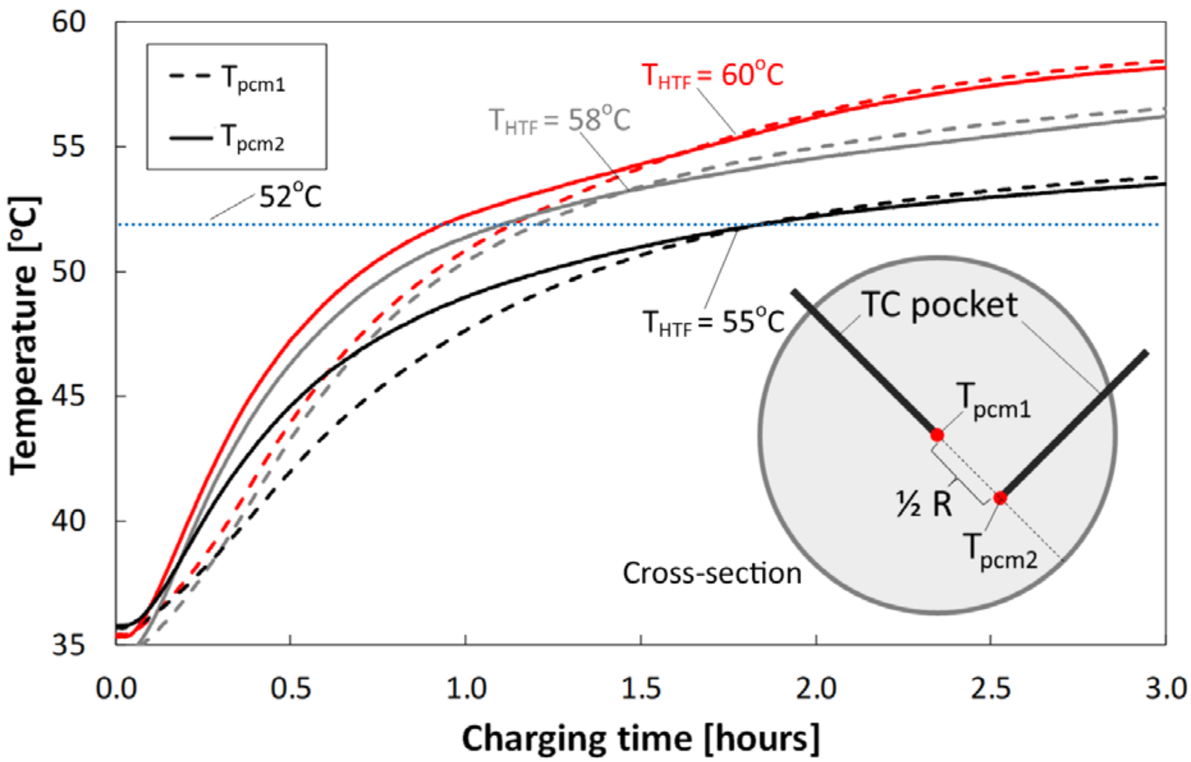

Figure 12: The evolution of PCM temperatures at two radial positions inside the PCM rods: charging in horizontal alignment.

In Figure 13, temperatures inside the PCM rod are plotted for four positions: T_{pcm1} and T_{pcm2} at one axial position in the lower part of rod, and T_{pcm3} and T_{pcm4} at another axial position at the upper part of the rod. T_{pcm1} and T_{pcm2} have the same radial positions as T_{pcm3} and T_{pcm4}.

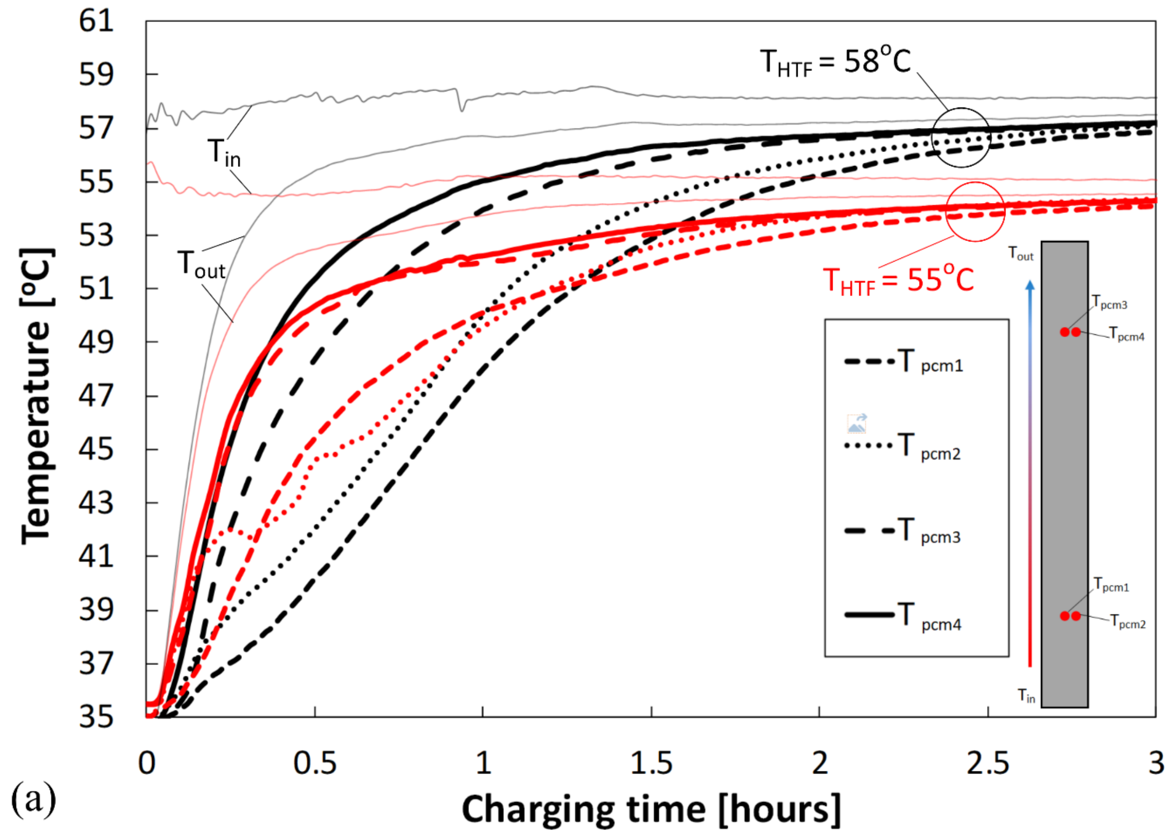

Figure 13: The evolution of PCM temperatures at two axial positions inside the PCM rods: charging in vertical alignment with upward HTF flow.

When the upward flow is supplied to the PCM-TES tank from the bottom, T_{pcm3} and T_{pcm4} at the upper part of the cylinder had values higher than T_{pcm1} and T_{pcm2} which are at the lower part of the rod, although the HTF temperature should be lower at the upper part of the rod than the lower. Such observations indicate the presence of natural convection of the PCM when melting inside the rod; i.e. the melted PCM travels vertically inside the rod. Furthermore, no crossing behavior is observed by the profile of T_{pcm1} and T_{pcm2}, unlike the one observed in the horizontal alignment. Therefore, although gelled PCM exhibits high viscosity and heat transfer mechanism has been regarded to be conduction-dominant, motion of melted PCM in cylinders is observed.

When the downwards flow of HTF is imposed, a larger temperature difference is observed in Figure 14 between PCM temperatures at the top (T_{pcm3} and T_{pcm4}) and those at the bottom (T_{pcm1} and T_{pcm2}) comparing to the mode of upward flow, especially with the HTF temperature at 58°C. Such observations could be due to that the upper region is melted more rapidly as being closer to the HTF's warm inlet and the liquid PCM tends to flow upwards instead of downwards because of the buoyant effect.

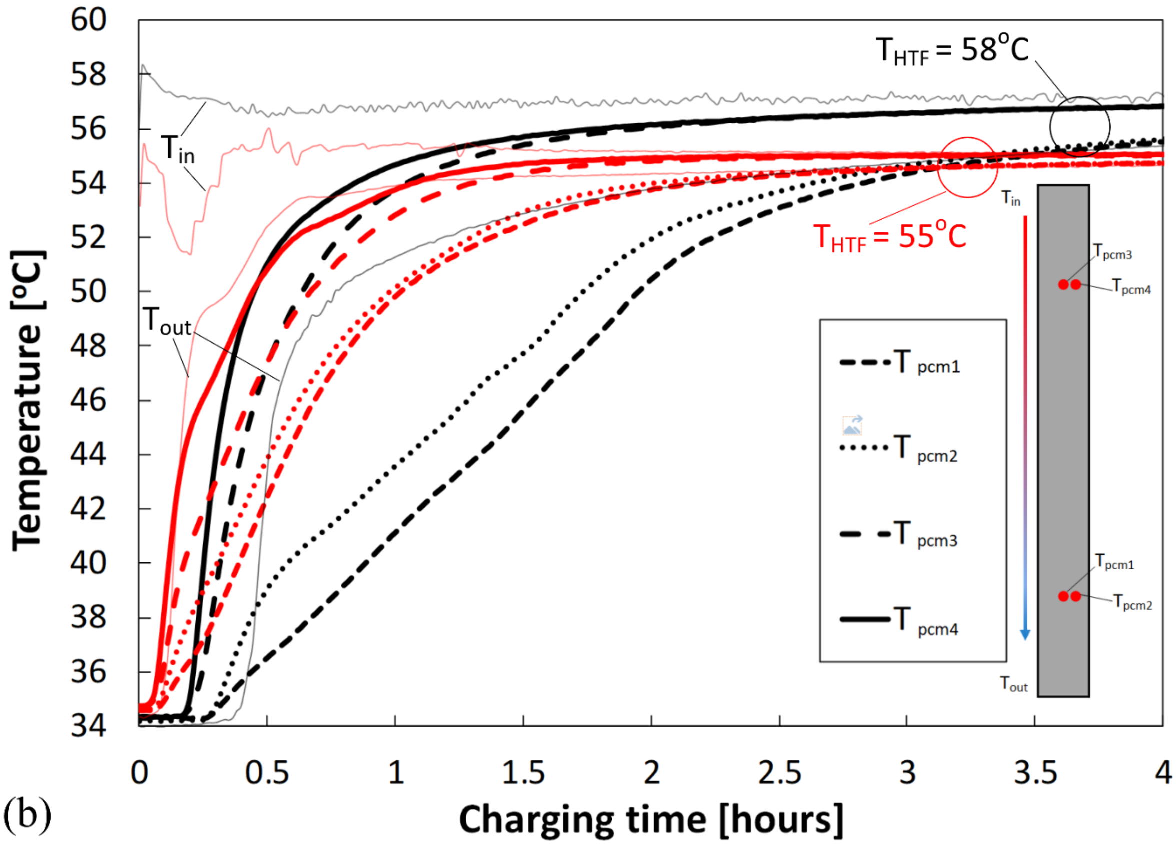

(b)

Figure 14: The evolution of PCM temperatures at two axial positions inside the PCM rods: charging in vertical alignment with downward HTF flow.

Temperature profile analysis: discharging

Natural convection is much less important in the solidification process than the melting and heat transfer in vertically-placed cylinders containing PCMs can be regarded as being dominated by heat conduction[10]. Such statements are found to be valid in the current experimental study in PCM cylinders.

In Figure 15, PCM temperature evolution along the axial direction of downward (red) and upward (black) flowing mode is shown. Both red and black curves show that during the first half hour when PCM is not solidified completely, T_{pcm3} and T_{pcm4}, are measured to be higher than T_{pcm1} and T_{pcm2} due to the stratification of liquid PCMs. However, after 1,5 hours when all measured temperature drop below 40^{o}C, the temperature difference becomes minor. T_{pcm1} and T_{pcm2} are lower in the upward flow mode because the water temperature at the same axial position on the cylinder, T_{w2}, is lower.

[10] Farid, M., et al., The Role of Natural Convection During Melting and Solidification of Pcm in A Vertical Cylinder. Chemical Engineering Communications, 1989. 84(1): p. 43-60.

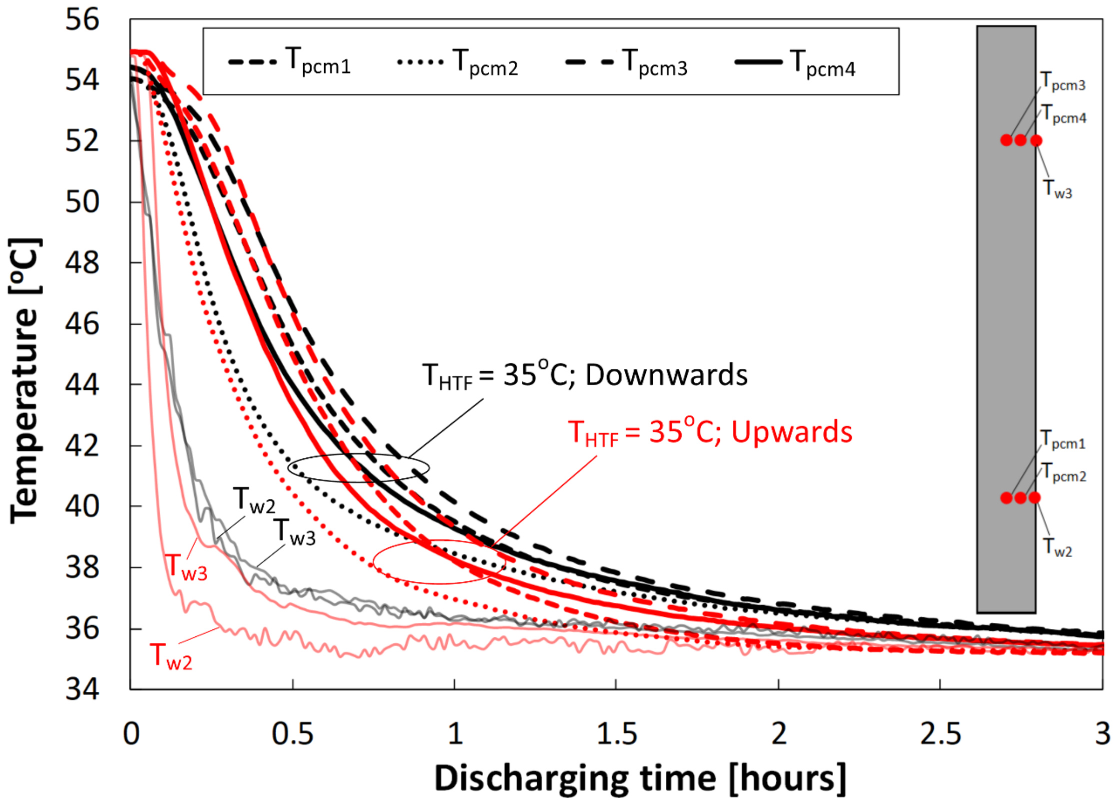

Figure 15: The evolution of PCM temperatures at two axial positions inside the PCM rods: discharging in vertical alignment with upward and downward HTF flow.

3.2.4 Conclusions of experimental analysis

The test rig for investigating the performance of PCM-TES tank over wide range of operating conditions has been built at the laboratory of the Energy Technology Department at KTH. The TES tank containing the PCM has also been designed and built. The test rig allows testing the PCM-TES tank over wide range of temperatures and volume flow rates of HTF; hence it was possible to characterize the performance of the PCM-TES tank.

Main conclusions from the experimental analysis done on the PCM ClimSel C48 in this project can be summarized as follows:

- Increasing the temperature difference between the phase-change temperature and the supply HTF reduces the time needed for charging and discharging. The tested PCM has peak phase change temperature of 48°C, it takes 5,6 hours to charge the PCM with 8 kWh with HTF supply temperature of 55°C but only 3,1 hours with that of 58°C. However, further increasing the HTF supply temperature to 60°C only reduces this time to 2,7 hours.

- Increasing the volumetric flow rate of the HTF improves the convective heat transfer over the encapsulation and reduces the charging/discharging time. However, the effect was not significant on charging/discharging time, the effect of temperature difference between HTF and PCM was more dominant.
- In the horizontal alignment the volume flow rate should be large enough to ensure uniform distribution of HTF over the rods; i.e. eliminate stratification. This was not a problem in vertical alignment where it was possible to operate at volume flow rates down to 0,15m^3/hr without degrading the performance of the PCM-TES tank. The low volume flow rate gives key advantage in leveled discharging power output and a higher outlet temperature from the PCM-TES tank in a longer discharging timespan.
  The pressure drop across the tank was measured to be negligible in all cases.
- Performance maps summarizing the completed test conditions over various HTF supply temperatures and volumetric flow rates have been generated. Charging maps indicate a non-linear increment of charging time when storing latent heat in PCMs above 75% of theoretical chargeable thermal capacity. The charging time can be significantly reduced by about 50% if 75% instead of 99% of the charged PCM thermal capacity is aimed for. The same trend is found in discharging processes.
- Conductive heat transfer was expected to be the dominant (or almost only) heat transfer mechanism in the gelled salt hydrates PCM. However, the temperature measurements inside the vertically aligned PCM rods indicate the presence of convection of melted PCMs.

Future work in the experimental analysis will include testing other PCMs, such as ClimSel C58, and characterize the performance of an optimized design of the PCM-TES tank. An optimized PCM-TES tank will most probably contain thinner PCM rods than tested in this project; other encapsulation geometries might also be tested.

The new PCMs to be tested will be chosen to cover other temperature ranges than tested in this project in order to cover wide range of applications where PCM-TES concept can be implemented.

3.3 Computer modelling

The experimental work in this project has been combined with computer simulation modelling. Modelling has been done at different levels:

- Modelling of the PCM-TES tank with the purpose of optimizing the tank design, example of optimization parameters are: size and shape of PCM, size and shape of the TES tank, HTF volume flow rate and its influence on heat transfer and pressure drop.
- Modelling of energy system with PCM-TES. The purpose of this analysis is to find an application where an energy system with PCM-TES gives large savings in energy and low payback time.

3.3.1 Modelling of thermal storage unit

The key component in the thermal storage unit is the PCM where the modelling focused. Simplified one and two dimensional models have been performed.

One dimensional analysis

One dimensional simplified model has been implemented which assumes only conduction heat transfer in the PCM rods. The specific heat transfer was assumed constant and averaged over the phase change temperature range. Table 3 is a summary of the results comparing the experimental results of charging/discharging time with the results of the one dimensional model.

Table 3: Comparison between experimental and one dimensional model charging/discharging time

Test conditions	Model time (h)	Experimental time (h)	Δtime (%)
melting 35 to 55, flow rate 1,5	4,611	4,326	6,59
melting 35 to 55, flow rate 4	4,179	1,969	112,24
melting 35 to 58, flow rate 1,5	4,771	4,195	13,73
melting 40 to 55, flow rate 1	4,499	7,113	36,75
melting 40 to 55, flow rate 1,5	4,252	5,712	25,56
melting 40 to 55, flow rate 2,5	4,018	3,290	22,13
melting 43 to 55, flow rate 1,5 (44 rods)	3,964	3,677	7,81
cooling 55 to 40, flow rate 1,5	4,173	6,579	36,57
cooling 55 to 35, flow rate 1,5	4,564	4,255	7,26

As can be observed in the table large differences can be found between the one dimensional model and some test conditions, which means that further refinement of the one dimensional model needs to be implemented, such as using curve fitting of specific heat of the PCM over the phase change temperature, instead of using an average value. It is also necessary to distinguish in the model between the regions where single and two phase heat transfer occur and use the corresponding material properties. In the current model, averages over the whole test period and temperature range have been used.

The material properties used in the models are based on the manufacturer data which should be verified that they match the properties of the materials used in the tests. Therefore, the properties of the PCM should be verified in our laboratories and reused in the calculation models if different from the manufacturer’s tables.

Two dimensional analysis

There have been various modelling studies using commercial CFD software, such as ANSYS FLUENT and COMSOL. These modelling tools give numerical solutions on properly defined phase-change problems which have been successfully validated by experimental results. Therefore, a two dimensional analysis using ANSYS FLUENT 17.1 was conducted in the project. The objective of this part of study is to model and investigate the phase-change processes focusing on following points: what is the main heat transfer mechanism during melting/solidification processes in cylindrically PCM encapsulations and how boundary conditions of cylinders affect heat transfer rate in PCMs.

The PCM that has been modelled in this part does not match the material or rod size that we experimentally investigated. The modelling in this part has been done in cooperation with colleagues in the thermal energy storage group at our department at KTH where their interest and ours have been merged in defining this case study, so we can all draw key conclusions and then we can modify the model to match our own individual research needs.

Modelling approach and quality control

Governing equation which are solved numerically in the model are continuity, momentum equation and energy equations. FLUENT applied a default numerical approach to solve phase-changing problems. This method is called enthalpy porosity method.

The quality of the model is validated by four means: residuals control, mesh independency test, time-step independency test and solution method independency test. The test results show that the created model shows good independency on the aforementioned settings regarding the liquid fraction. Therefore, the quality of the model is validated.

Modelled results

An organic commercial PCM (RT35) with a phase-change temperature at around 35^{o}C was modelled in the present study. Visualization of melting and solidification process is shown in Figure 16. It is observed that during the melting the natural convection in PCM domains redistributes the temperature gradient and liquid PCMs tend to flow upwards due to the buoyant effects. However, for solidification the heat transfer mechanism is conduction-dominant, as the temperature uniformly decreases from the core to the edge.

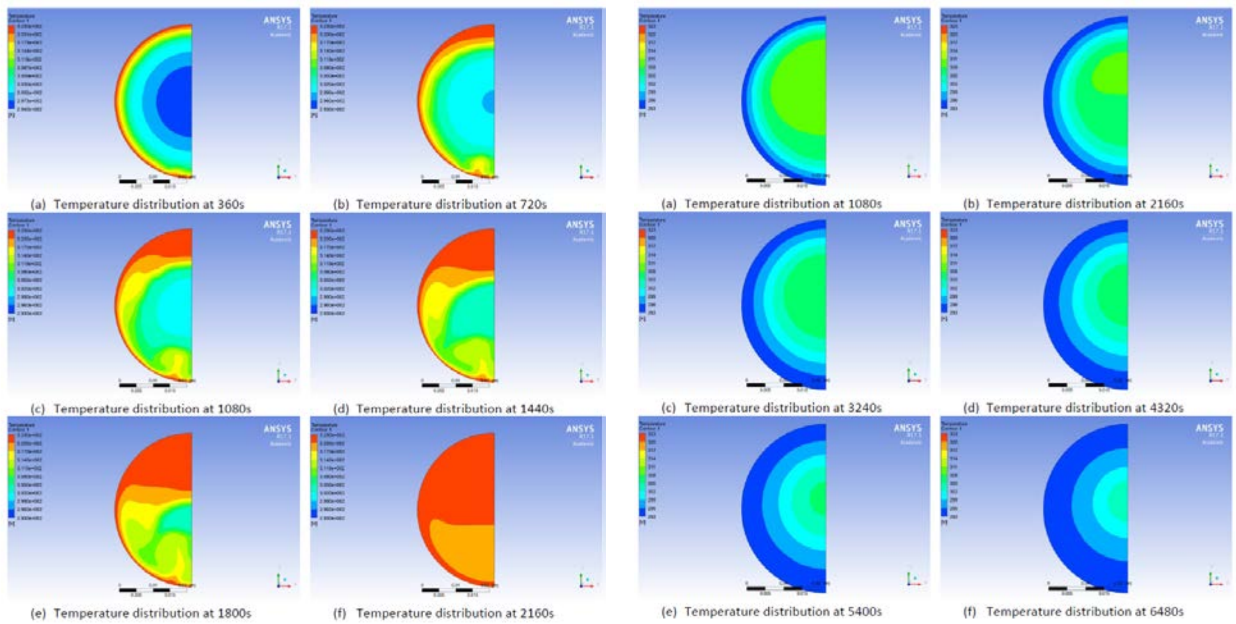

(a) Melting process with 50 ^{o}C at the boundary (b) Solidification process with 20 ^{o}C at the boundary

Figure 16 Temperature distribution in PCM cylinders of melting and solidification

In the parametric study, different temperature boundary conditions (50^{o}C, 60^{o}C and 70^{o}C for melting; 20^{o}C, 10^{o}C and 0^{o}C for solidification) were set along the perimeter of a cylinder on a two-dimensional basis. In Figure 17, the status of phase-change is expressed in terms of the liquid fraction, which equals to 1 when PCMs are completely melted and equals to 0 when completely solidified. The modelled results reveal that increasing the difference between the phase-change temperature and the boundary temperature accelerates the heat transfer rates and reduce the melting/solidification time.

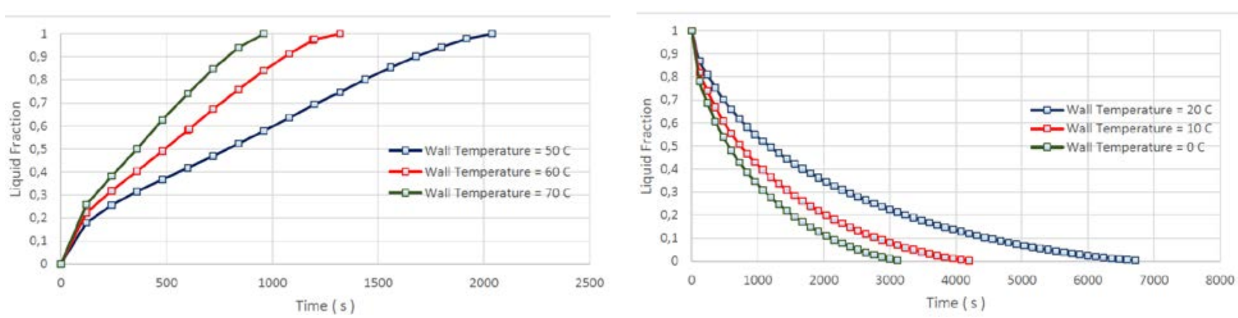

(a) Melting with 50, 60, 70^{o}C at the boundary (b) Solidification with 20, 10, 0^{o}C at the boundary

Figure 17 Liquid fraction with different boundary temperatures

The two-dimensional analysis shows: Firstly, the natural convection was observed in melting processes but not in the solidification process. Secondly, raising the temperature difference as an improved driving force of phase-change process reduces the required melting/solidification time.

3.3.2 Modelling of energy system with PCM

The target application for the PCM-TES was identified as space heating in residential applications where single family house was selected to demonstrate the potential of the concept. The case of a single family house offers simplicity in system dynamics and the possibility to generate representative load profiles. An ASHP providing the space heating needs for the single family house possess characteristics which can benefit from the advantages of PCM-TES. The performance of an ASHP, i.e. capacity and efficiency, is strongly dependent on the outdoor temperatures, where at low outdoor temperatures the heat pump loses in capacity and efficiency. Therefore, it is possible to operate the heat pump for thermal storage during the high efficiency and capacity periods of the day and utilize the stored heat for space heating when the outdoor temperature is low.

This operation strategy is expected to result in the lowest energy use possible with PCM-TES; however, taking the varying electricity prices during the day the ASHP can be controlled to avoid running at high prices during the peak hours. In this operation strategy the ASHP is operated to store energy in the PCM-TES tank during the off-peak hours with low electricity prices and discharge the stored energy when the prices are high; i.e. reduce running time of the heat pump at peak loads.

Air source heat pump with PCM-TES

The layout of a common hot water radiator system in typical Swedish single-family dwellings is proposed in Figure 18. The heating is provided by a state-of-the-art variable-speed ASHP using propane as the refrigerant. Propane has been selected because it is a natural refrigerant with a good potential to be widely used in ASHP for single family houses. The PCM-TES tank, indicated as (2) in Figure 18, can be charged by the warm water loop connected to the ASHP. The heating load in the house can be fulfilled by: the ASHP only, discharging the PCM-TES tank only, or the simultaneous operation of the ASHP and discharging PCM-TES tank.

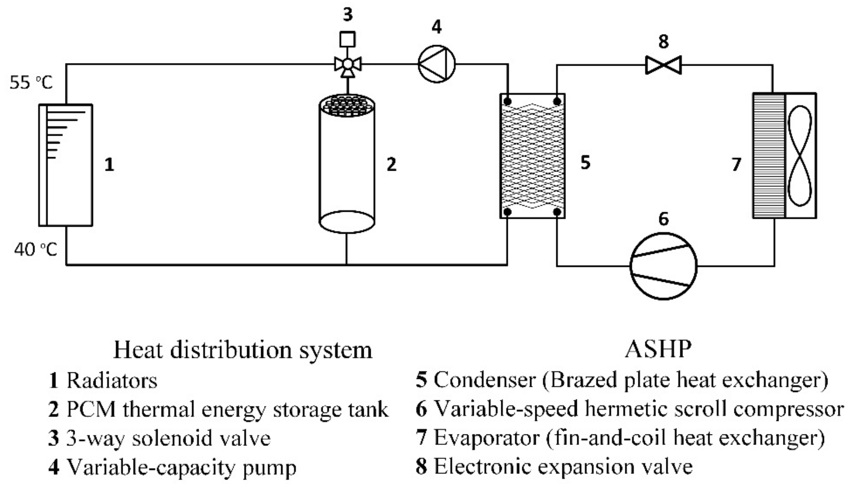

Figure 18: Schematic layout of ASHP for space heating with integrated PCM-TES tank.

The load profiles for the a single family house in Sweden has been generated and used in calculating the energy use of the ASHP in two main operation strategies: targeting minimizing energy use, or minimizing running cost.

The performance of the ASHP was characterized based on experimental studies carried out in earlier project but published in this project due to its relevance. The performance of the PCM-TES tank is characterized by the experimental studies carried out in this project and assumed to have a thermal storage capacity of 9,5 kWh.

<u>Minimum energy use operation strategy</u>

The space heating load profile for a single family house and the electric tariff variation during the day are plotted in Figure 19. The selected day is the 1st of March 2018 where the outdoor temperature varied between -18°C during night and -6°C during the day. The shifted thermal capacity is highlighted in Figure 19, which can be noticed as the difference between the demand and the heat provided by the heat pump.

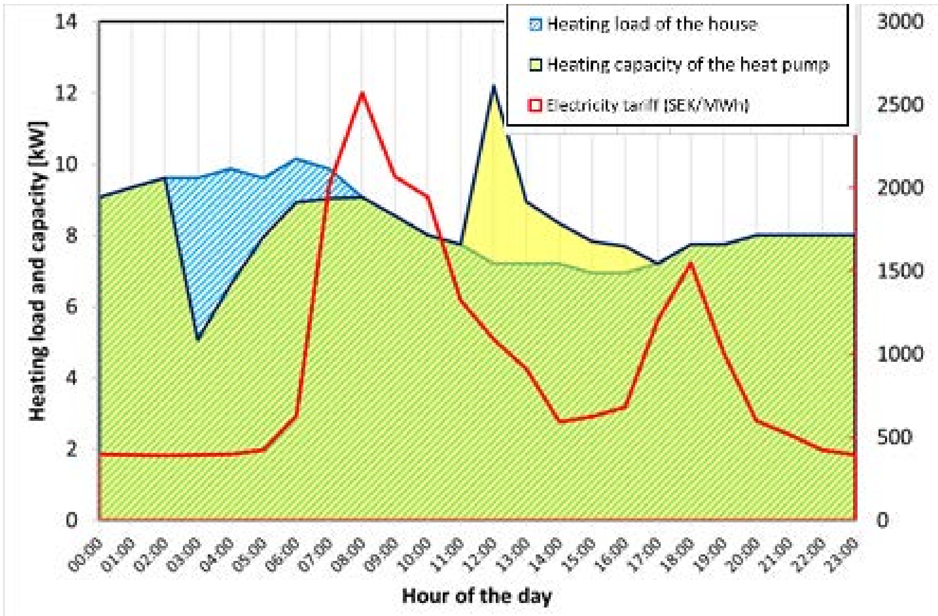

Figure 19: Hourly heating load, charged/discharged capacity, and electric tariff over a day- Minimum energy use operation strategy.

The energy use of the house is reduced to 7% by implementing the load shifting in the studied day, a strong factor in this saving is that the heat pump was assumed to be switched off at outdoor temperatures lower than -15°C and the auxiliary electric heater was used to provide all the heating needs. However, since the electricity tariff was low during the time the heat pump was switched off the system did not save much in the energy cost, about 3%.

Minimum cost of energy operation strategy

The control strategy to reduce energy cost of running the system can be observed in the plots in Figure 20. The load in this case has been shifted from the peak hours where the electricity cost is high, i.e. during the morning hours, to the period where the cost is low during night.

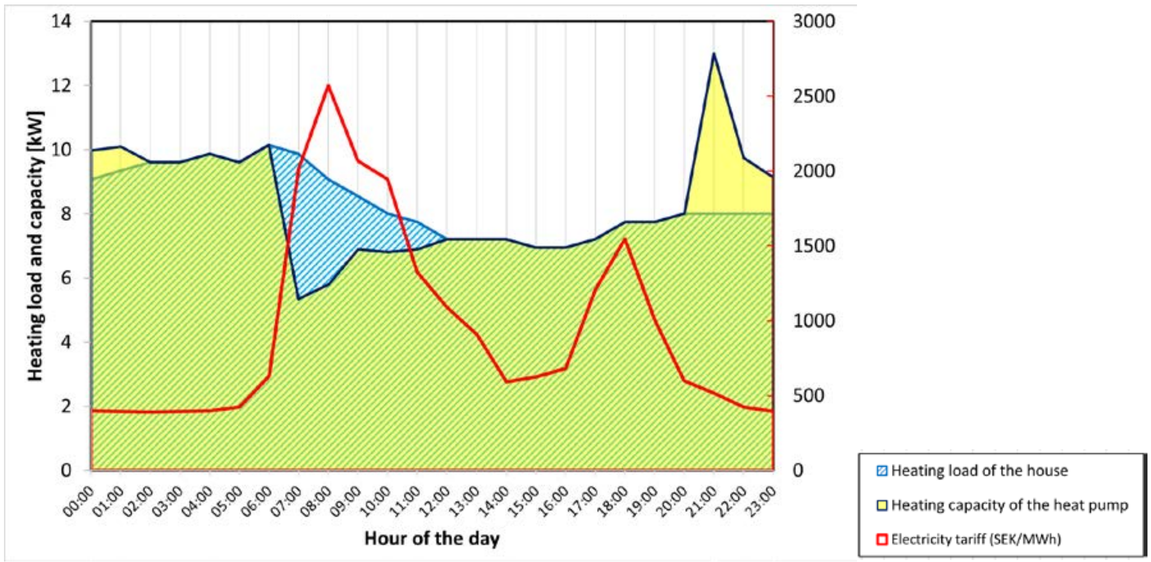

Figure 20: Hourly heating load, charged/discharged capacity, and electric tariff over a day-Minimum cost of energy operation strategy.

The analysis is done for the same day as in the minimum energy use operation strategy; 1st of March 2018. The energy use of the system with load shifting in this operation strategy was negligible, but since the ASHP was running at lower capacity during the peak hours the energy cost of running the system for that day was reduced by about 9%.

Since this operation strategy is not based on the heat source temperature that gives the highest heat pump efficiency the ground source heat pump may have a good potential for energy cost savings, might be even higher than in this studied case of the ASHP.

Air source heat pump with PCM-TES at de-superheater

One of the key factors that limit the environmental and financial gains from the PCM-TES tank in the ASHP system for space heating is that the PCM-TES tank needs to be charged at higher temperature relative to the temperature level that needs to be supplied to the heating system. For example, in the tested PCM-TES tank in this project, the HTF supply temperature should be at least 58°C while discharging can be achieved at temperatures lower than 40°C.

An alternative arrangement that may improve the performance of heat pump systems with PCM-TES is to take the heat from the heat pump using two separate heat exchangers:

- de-superheater for hot supply temperature to PCM-TES tank
- and condenser for space heating

This is a typical arrangement for heat pump providing heat for domestic hot water and space heating simultaneously. The proposed layout is presented in Figure 21.

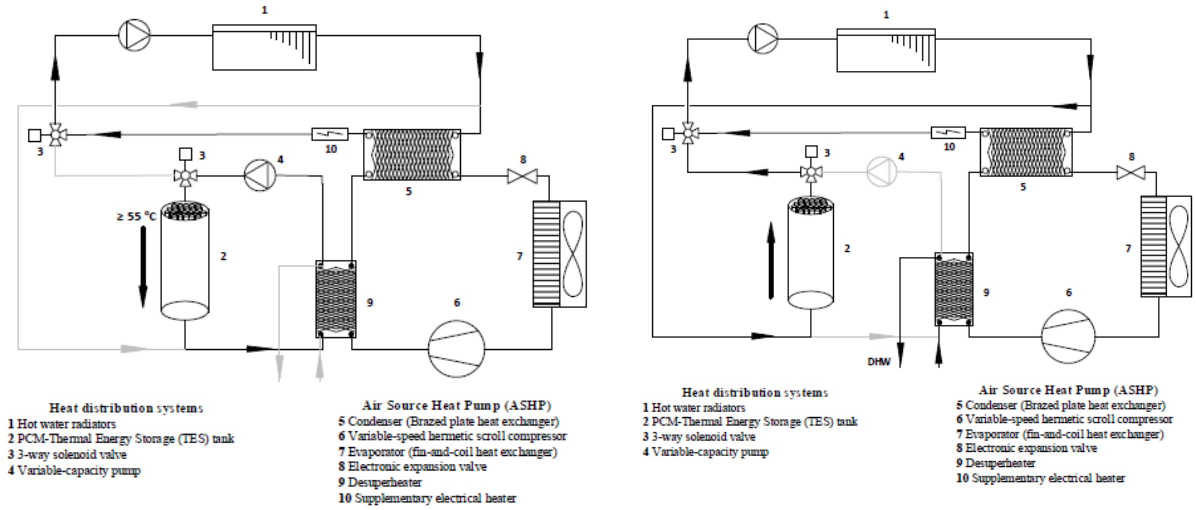

Figure 21: Schematic layout of ASHP providing space heating from the condenser with integrated PCM-TES tank connected to de-superheater (right) discharging (left) charging

As can be observed in the plot to the left in Figure 21, the PCM-TES tank can be charged with relatively high temperature whenever the heat pump is running to cover the space heating demand. When the PCM-TES tank is sufficiently charged it can be discharged according to the configuration in the right plot in Figure 21, this can be done during the period of the day that gives the best environmental and/or economical effect; i.e. low energy use or cost.

The proper match between the capacities and the level of temperature needs in the condenser and the de-superheater is essential to obtain high efficiency from this system arrangement. Analysing experimental and modelling results from previous study on propane ASHP, the condensing temperature and the heating COP of the heat pump remained almost constant when heat is recovered from the two heat exchangers arrangement. This can be seen in the plots presented in Figure 22.

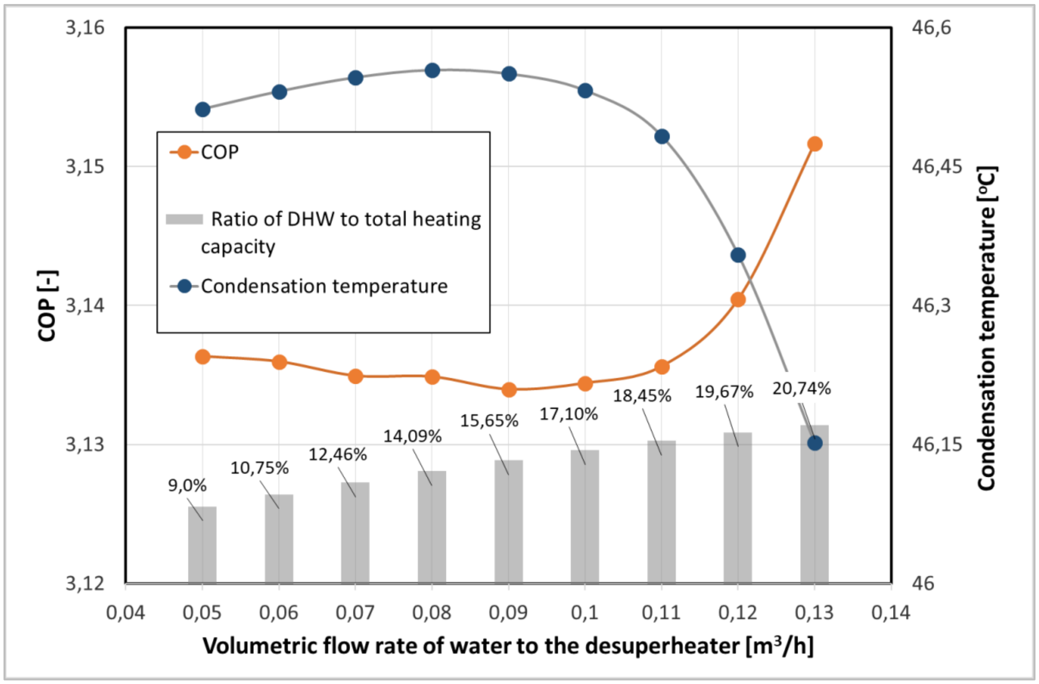

Figure 22: Heating COP, condensing temperature, and capacity ratio of DHW to total heating at different volume flow rates in the de-superheater of ASHP

The energy use or cost for the ASHP system when connecting the PCM-TES tank to the de-superheater was not calculated in this project; but the performance of the heat pump presented in this section shows that there is a good potential for increasing the energy and cost savings.

3.3.3 Conclusions of modelling analysis

One and two dimensional analysis has been conducted to simulate the melting and solidification process of the PCM rods. The simplified one dimensional model had good agreement with some of our experimental data, but large differences were observed with some other points. This highlights the need for refining the model by introducing the thermosphysical properties of PCM as a function of temperature instead of using averages over a wide temperature range. The thermophysical properties of the PCM will need to be obtained in our laboratories to make sure that it matches the provided values from the manufacturer.

The quality of the two-dimensional model has been validated and compared to experimental and modelling values in literature. The PCM that has been modelled in the two dimensional model does not match the material we experimentally investigated. The model has to be modified to match the conditions and characteristics of our own case.

A proposed application for the PCM-TES is a heating system with ASHP for space heating in a single family house. The possible savings by using the PCM-TES have been modelled for two scenarios: minimum energy cost and minimum energy use. When the system is controlled to shift loads to minimum energy cost in a selected day, about 9% reduction in energy cost has been calculated for that day; however, energy use remained almost unchanged. When the system is controlled for the lowest energy use about 7% reduction in energy use was calculated; however, in this case the reduction in cost was only 3%.

The calculations show a good potential for savings in energy use or energy cost, further savings can be expected by improving the system design which can be achieved by connecting the PCM-TES tank to the des-superheater of the heat pump. This will allow providing high HTF temperature to the PCM-TES tank at the same time as the heat pump provides the required space heating. The heating COP of the heat pump in this arrangement remains almost constant; i.e. no need to raise the condensing pressure which reduces the heating COP.

3.4 Discussions and future work

3.4.1 Discussions

The test rig for investigating the performance of PCM-TES tank over wide range of operating conditions has been built at the laboratory of the Energy Technology Department at KTH. The TES tank containing the PCM has also been designed and built. The test rig allows testing the PCM-TES tank over wide range of temperatures and volume flow rates of HTF; hence it was possible to characterize the performance of the PCM-TES tank.

One PCM has been tested with a test matrix of 29 points where each test took about 10 hours to accomplish. The tests gave complete characterization of the PCM-TES tank with performance map that can be used for PCM-TES tank sizing and efficient integration into the relevant energy system/s. The key influencing parameters on the performance of the PCM-TES tank have been identified and included in the performance map.

In addition to the already obtained research results, the testing equipment and the analysis methods (experimental and modeling) that have been established in this project are important outcomes. This powerful research infrastructure can be used in the future as a platform for modelling and testing new PCMs and TES tank configurations.

3.4.2 Future work

The work in this project can be seen as an important start for future work in this area. Additional work will be needed to characterize the performance of more PCMs and TES geometries. The tools developed in this project can also be used to optimize the design of the PCM-TES tank, for example, the PCM rods that have been used in this project have been off-the-shelf for large applications; however, smaller rods are expected to produce lower charging/discharging time.

The performance maps that have been generated in this project can be used for optimizing the performance of the energy systems with PCM-TES tank. Higher HTF supply temperature will require additional energy from the energy system and the increasing volume flow rate will consume pumping power, the optimum operating condition should be obtained. Also it should be possible to calculate at which PCM-TES charging/discharge capacity (in percentage) the energy system should aim for to achieve the highest savings.

The material properties used in the models in this project are based on the manufacturer data which should be verified that they match the properties of the actual materials used in the tests. Therefore, the properties of the PCM should be verified in our laboratories and reused in the calculation models if different from the manufacturer's tables.

The one dimensional model will need to be refined by using the specific heat as a function of temperature instead of using an average value. It is also necessary to distinguish in the model between the regions where single and two phase heat transfer occur and use the corresponding material properties.

The two dimensional model should be modified to implement the properties of the PCM uses in our experiments; hence the modelling results can be compared to the experimental. The verified two dimensional model can then be used to optimize the design of the PCM-TES tank.

An interesting application for the PCM-TES is to use it in an energy system with ASHP for space heating. More detailed modelling is needed in order to evaluate the savings in annual energy use. The potential improvement on energy efficiency with connecting the PCM-TES tank to the des-superheater of the heat pump needs to be invistigated. This will allow providing high HTF temperature to the PCM-TES tank at the same time as the heat pump provides the required space heating. The heating COP of the heat pump in this arrangement remains almost constant; i.e. no need to raise the condensing pressure which reduces the heating COP.

4 Publications list

The project publications are listed below. The contribution of the key publications to the project activities and objectives is clear in the results chapter.

Journal papers:

Due to the limited time frame of the project and generating the results at the later phase of the project no journal papers have been published. However, at least one journal paper will be published based on the experimental results that have been obtained in this project.

The PhD student Tianhao Xu will continue working on this topic for his PhD studies for at least one more year and will include some of the project results in his research publications. For example, the performance of ASHP with PCM-TES tank connected at the de-superheater will be developed into journal paper.

Conference papers:

3 in total: 2 published, 1 accepted to be published in August 2018:

1. Xu T. and Sawalha S., Space Heating Systems Integrating Heat Pumps and PCM Thermal Energy Storage Units in Swedish Single-family Houses: A Case Study. International Conference on Cryogenics and Refrigeration, April, 2018, Shanghai, China.
2. Xu T., Navarro-Peris E., Piscopiello S., Sawalha S., Corberán J. M., and Palm B., Large-Capacity Propane Heat Pumps for DHW Production in Residential Buildings. 13th IIR Gustav Lorentzen Conference, Valencia, June 2018.
3. Xu T., Sawalha S., and Palm B., Experimental Investigations on a Thermal Energy Storage Unit Using Tubular Encapsulated PCMs for Space Heating Applications, 10th International Conference on Applied Energy (ICAE2018), 22-25 August 2018, Hong Kong, China. Accepted for publication.

Master thesis:

1. Loris Tomasi, Experimental investigations of a thermal storage unit using phase change materials (PCM) for space heating applications, presented on 24^{th} of April 2018. Report will be available after the summer of 2018.
2. Konstantinos Papiris, Modelling of different configurations of thermal energy storage tanks with phase change materials. Will be presented on the 22^{nd} of August 2018. Report is expected in September 2018.

3. Hasnain Raza, Heating and cooling systems of residential buildings with thermal energy storage using phase change materials (TES-PCM). Will be presented on the 22nd of August 2018. Report is expected in September 2018.

Technical magazine:

1. Xu T. and Sawalha, S., Korttidslagring av energi med fasändringmaterial för effektiv integrering med värme- och kylsystem i byggnader-Effsys Expand projekt på KTH. Kyla & Värme, 2016.

Presentations and conference presentations:

- Poster presentation oral presentations at:
    - Svenska Kyl & Värmepumpdagen- 20 October 2017, Stockholm
    - Svenska Kyl & Värmepumpdagen- 21 October 2016, Göteborg
    - Effsys Expand forskardagar, 16 May 2016, Tranås, Sweden
    - Effsys Expand forskardagar, 17 April 2018, Tranås, Sweden

5 References

Detailed references can be found in the project publications.

6 Appendix

1. Conference paper I
2. Conference paper II
3. Conference paper III